JACC: BASIC TO TRANSLATIONAL SCIENCE VOL. ■, NO. ■, 2025

ORIGINAL RESEARCH - PRECLINICAL

Small Interfering RNA Therapy Targeting the Long Noncoding RNA SMILR for Therapeutic Intervention in Coronary Artery Bypass Graft Failure

Simon D. Brown, PhD,[a] Anna L. Malinowska, PhD,[b] Matthew Bennett, PhD,[a] Andrés F. Correa-Sánchez, MSc,[b] Laia Linda Horcasitas Valencia, BSc (Hons),[a] Aimee P. Lucignoli, MSc,[c] Anna K. Barton, MD,[a] Laura Clark, MD,[a] Judith C. Sluimer, PhD,[a,d] Scott P. Webster, PhD,[a] Julie Rodor, PhD,[a] David E. Newby, MD, PhD,[a] Mark Cunningham, BSc (Hons),[b] Andrew H. Baker, PhD[a,d]

VISUAL ABSTRACT

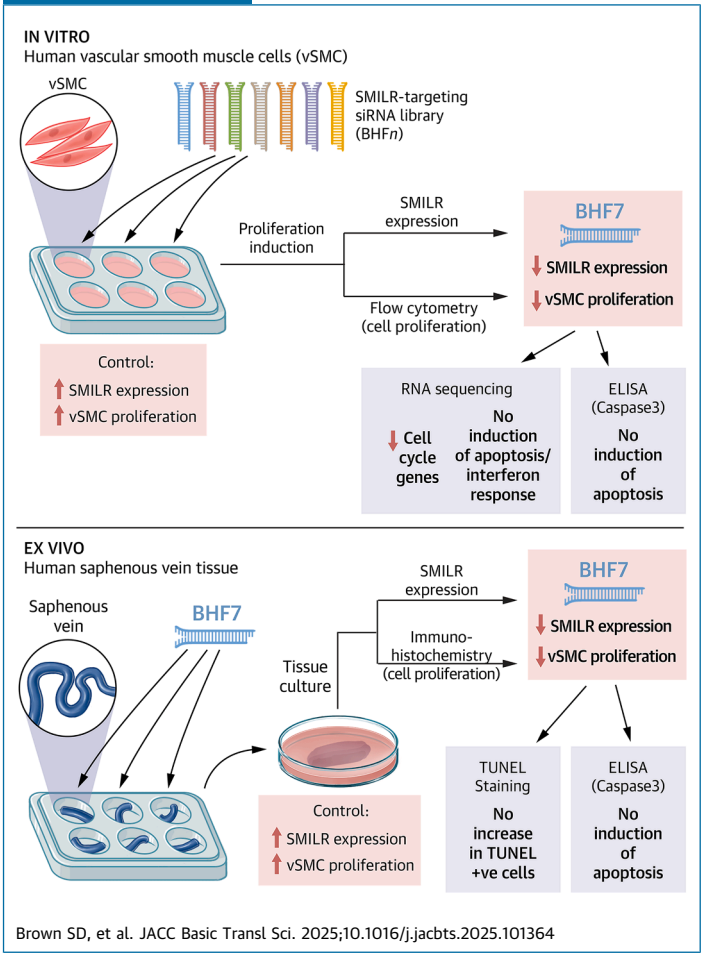

Brown SD, et al. JACC Basic Transl Sci. 2025;10.1016/j.jacbts.2025.101364

HIGHLIGHTS

- **Excessive vSMC proliferation is an important phenotype of CABG surgery failure.**
- **We previously identified SMILR as a human-specific long noncoding RNA that is expressed in proliferating vascular smooth muscle cells.**
- **We generated a library of siRNA molecules targeting the SMILR sequence to degrade the SMILR transcript and reduce pathologically induced vSMC proliferation.**
- **From this library, we identify BHF7 as an effective siRNA, which reproducibly demonstrates the ability to block SMILR expression and limits cell proliferation both in vitro and in a human *ex vivo* saphenous vein tissue model.**
- **RNA-sequencing of BHF7-treated vSMCs demonstrates widespread reductions in transcripts of genes with functions related to cell proliferation and mitosis.**
- **Transfection of BHF7 both in vitro and ex vivo did not induce a cytotoxic response, suggesting that delivery of BHF7 to patient tissues should be well-tolerated.**

ISSN 2452-302X https://doi.org/10.1016/j.jacbts.2025.101364

ABBREVIATIONS AND ACRONYMS

CABG = coronary artery bypass graft

EdU = 5-ethynyl-2′-deoxyuridine

IL1-alpha = interleukin 1 alpha

MYH11 = myosin heavy chain 11

PDGF = platelet-derived growth factor

qRT-PCR = quantitative real-time polymerase chain reaction

SMILR = smooth muscle induced long noncoding RNA

UBC = ubiquitin C

vSMC = vascular smooth muscle cell

SUMMARY

Coronary artery bypass graft (CABG) surgery remains the gold standard of care to prevent myocardial ischemia in patients with advanced atherosclerosis; however, poor long-term graft patency remains a considerable and long-standing problem. Excessive vascular smooth muscle cell (SMC) proliferation in the grafted tissue is recognized as central to late CABG failure. We previously identified SMILR, a human-specific SMC-enriched long noncoding RNA that drives SMC proliferation, suggesting that targeting SMILR expression could be a novel way to prevent neointima formation, and thus CABG failure. Here, we sought to identify a lead siRNA for clinical development. We describe the design and synthesis of a library of 76 chemically enhanced SMILR-targeting siRNA. From this library, we identify a lead siRNA, BHF7, which demonstrates potent and reproducible silencing of *SMILR* expression, and which robustly blocks vascular smooth muscle cell proliferation, both in vitro and in the ex vivo human saphenous vein model. We further demonstrate using RNA-sequencing that BHF7 down-regulates the expression of genes associated with proliferation and does not induce the expression of interferon or apoptosis genes, suggesting it has a favorable safety profile, both on- and off-target. Finally, we performed TUNEL staining on BHF7-treated tissues and measured the levels of cleaved caspase-3 by enzyme-linked immunosorbent assay after BHF7 treatment. This demonstrated that BHF7 does not induce a cytotoxic response either in vitro or ex vivo. Collectively, these data represent a preclinical package into the function and specificity of BHF7 which warrants further investigation into the possibility of utilizing BHF7 as a novel, ex vivo RNA therapeutic for the prevention of CABG failure in humans. (JACC Basic Transl Sci. 2025;■:101364)

Coronary artery bypass graft (CABG) surgery, particularly those using the great saphenous vein, remains the most commonly performed surgical intervention in patients with severe atherosclerosis.[1] Neointimal hyperplasia in the saphenous vein graft is the commonest cause of late CABG surgery failure.[2] It develops because of the maladaptive remodeling of the grafted tissue in response to iatrogenic damage and ischemia-reperfusion injury arising from excision of the tissue, and the high-pressure environment of the arterial circulation in which the vein needs to adapt after engraftment. This leads to, amongst many other responses, the phenotypic switching of vascular smooth muscle cells (vSMCs) from a quiescent to proliferative, promigratory, "synthetic" state, promoted by the increased exposure of vSMCs to proinflammatory mediators and cytokines such as interleukin-1α (IL1α) and platelet-derived growth factor (PDGF).[3,4] Over time, this excessive proliferation leads to an accumulation of vSMCs in the wall of the grafted vessel which occludes blood flow and results in an accelerated atherosclerosis-like process.[5,6] Left untreated, occlusion of the graft can lead to myocardial ischemia, angina pectoris, myocardial infarction, and death.

Clinical studies have shown that in the first year following surgery, 10% to 20% of bypass grafts are no longer patent,[7-13] and 5 to 10 years postgrafting, this failure rate can be as high as 50%.[7-9,14-21] Current therapeutic strategies depend on various factors including the degree of occlusion, comorbidities and the associated benefit of repeated intervention to the patient.[22] The options range from percutaneous coronary intervention to the grafted tissue,[23] where long-term outcomes remain very low,[24-26] redo CABG surgery, which is seldom performed,[27,28] or pharmacological management.[22] These treatment strategies

From the [a]BHF Centre for Cardiovascular Science, Queens Medical Research Institute, University of Edinburgh, Edinburgh, United Kingdom; [b]MRC/UKRI Nucleic Acid Therapy Accelerator (NATA), Research Complex at Harwell (RCaH), Harwell, Oxford, United Kingdom; [c]School of Biosciences, Cardiff University, Cardiff, United Kingdom; and the [d]Department of Pathology, Cardiovascular Research Institute Maastricht (CARIM), Maastricht University Medical Centre, Maastricht, the Netherlands.

The authors attest they are in compliance with human studies committees and animal welfare regulations of the authors' institutions and Food and Drug Administration guidelines, including patient consent where appropriate. For more information, visit the Author Center.

Manuscript received May 2, 2025; revised manuscript received July 10, 2025, accepted July 22, 2025.

have remained largely ineffective meaning bypass graft failure rates have remained unchanged for several decades.[29]

Long noncoding RNAs have emerged as key regulators of various physiological and, importantly, pathophysiological processes, including in vSMCs.[30] We previously identified and characterized smooth muscle-induced long noncoding RNA (SMILR)—a human-specific long noncoding RNA that becomes expressed in vSMCs following pathological stimulation with interleukin (IL)-1 and platelet-derived growth factor (PDGF).[31] Importantly, SMILR expression is not induced in vascular endothelial cells after stimulation with IL1 and PDGF, suggesting that SMILR has vSMC-specific functions in response to pathological stimulation. Both IL1 and PDGF are known to induce proliferative pathways in vSMCs and play key roles in the development of vein graft failure,[3,32-34] leading us to hypothesize that SMILR may act to promote vSMC proliferation. Further mechanistic studies established that SMILR binds to the mRNA of the cell cycle protein centromere protein F (CENPF) and to the RNA-binding protein Staufen1 (Stau1), known for its role in nonsense-mediated decay.[35] Through its binding, SMILR shields CENPF from Stau1-mediated degradation, thus promoting vSMC proliferation. SMILR is therefore a key driver of proliferation specifically in vSMCs with no apparent expression in vascular endothelial cells, and by being expressed early after pathological stimulation and acting to drive proliferation, is thus a key mediator of venous bypass graft failure.[31,36] The nature of CABG surgery lends itself to ex vivo therapeutic approaches as the saphenous vein tissue is removed from the leg and sits outside the body for approximately 30 minutes before grafting onto the aorta and coronary circulation. Therefore, there exists a clinical window in which a therapeutic intervention can be delivered to the tissue, providing localized delivery. We substantiated the translational potential of targeted SMILR knockdown through the use of a simple, commercially obtained short interfering RNA (siRNA), which was effective in vitro at reducing vSMC proliferation and showed promising results in an ex vivo saphenous vein remodeling system.[36] It is also worth noting that, as a long noncoding RNA, targeting SMILR with a short oligonucleotide presents several advantages over the use of more standard small and large molecule therapeutic interventions.[37]

Here, we develop the translational potential of targeted SMILR knockdown by describing the development and characterization of a library of chemically enhanced double-stranded siRNA compounds targeting different regions of the SMILR transcript. We sought to develop a lead siRNA for clinical development. We designed and synthesized 76 SMILR-targeting siRNAs (BHF_n) and a nontargeting control siRNA (siNTC), and transfected each into saphenous vein smooth muscle cells derived from surplus tissues taken from patients undergoing CABG surgery. We then assessed SMILR expression and vSMC proliferation after transfection and stimulation of vSMCs with IL1 and PDGF. We then defined one of these siRNAs, BHF7, as the lead siRNA which reproducibly demonstrated maximal SMILR knockdown and cessation of proliferation both in vitro and ex vivo in the human saphenous vein model. Deep RNA-sequencing of BHF7-treated vSMCs revealed widespread reductions in the expression of a cell-cycle associated gene network without induction of interferon or apoptosis genes, suggesting that implantation of BHF7-treated saphenous veins in patients should be efficacious. Finally, when delivered either in vitro to cells or ex vivo to saphenous vein tissue, BHF7 demonstrates no changes in cell membrane integrity, apoptosis or DNA fragmentation. BHF7 thus represents a novel siRNA therapeutic which can be delivered to saphenous vein tissue ex vivo during autologous bypass graft surgery in cardiac theatre with minimal change to surgical practice, and which has the potential to improve vein graft patency.

METHODS

DECLARATION OF HELSINKI. All studies were conducted in accordance with the Declaration of Helsinki, research ethics committee approval (East of Scotland Research Ethics Committee, 15/ES/0094) and the written informed consent of all subjects.

siRNA COMPOSITION. Each strand of the siRNA was 19 nucleotides long, with the antisense strand carrying a phosphate at the 5′-end and a 2 nucleotide deoxythymidine overhang at the 3′-end (Supplemental Figure 1A). An Enhanced Stabilisation Chemistry modification pattern[38,39] with some minor changes was utilized in which the 2′-OH position of the ribose is replaced by 2′-*O*-Methyl or 2′-fluoro modification. When placed across the siRNA, these modifications are reported to improve resistance to endonuclease digestion and enhance target affinity.[40] Additionally, 2 phosphorothioate bonds, in which an unbridged oxygen atom in the backbone is replaced with a sulfur, were introduced at both ends of the duplex to increase stability against exonucleases. All siRNA sequences are given in Supplemental Table 1.

SOLID PHASE OLIGONUCLEOTIDE SYNTHESIS. Oligonucleotides for screening were synthesized on a 50-nmol scale on the MerMade192X synthesizer (LGC Biosearch Technologies) or 1-μmol scale with the MerMade12 synthesizer (LGC Biosearch Technologies) using 1000 Å Universal Controlled Pore Glass (CPG) (loading 47.7 μmol/g, LGC Biosearch Technologies). Cleavage of the 4,4′-dimethoxytrityl (DMTr) group was performed with 3% trichloroacetic acid in dichloromethane (DCM) (LGC Biosearch Technologies). 2′-*O*-methyl phosphoramidites, 2′-fluoro phosphoramidites, dT phosphoramidite (with standard protecting groups) and 5′-phosphate phosphoramidite were prepared as 0.15 mol/L solutions (0.08 mol/L solutions for 1-μmol scale synthesis on the MerMade12 synthesizer) in dry acetonitrile (ACN) (LGC Biosearch Technologies). Solvents were moisture controlled with <30 ppm water content. 0.25 mol/L solution of 5-ethylthio-1*H*-tetrazole in dry ACN (LGC Biosearch Technologies) was used as an activator. Sulphurization was performed with 0.05 mol/L solution of EDITH (LGC Biosearch Technologies) in ACN. Failed sequences were capped with a 1:1 mixture of Capping Mix A (tetrahydrofuran/lutidine/acetic anhydride, 8:1:1, v/v/v, LGC Biosearch Technologies) and Capping Mix B (16% *N*-methylimidazole in tetrahydrofuran, LGC Biosearch Technologies). The oxidizing step was performed with 0.02 mol/L iodine in tetrahydrofuran/pyridine/water (7:2:1, v/v/v, LGC Biosearch Technologies).

BHF7-2, BHF7-3, BHF7-4, and Cy3-BHF7 were ordered from Biotage and quality controlled (Liquid Chromatography-Mass Spectrometry) and duplexed internally.

CLEAVAGE AND DEPROTECTION OF OLIGONUCLEOTIDES. Cleavage from the solid support: cleavage solution (200 μL of 32% aq ammonia and 40% methylamine [AMA] mixture) was added to the columns containing CPG. Then, a vacuum was carefully applied to pull the cleavage solution onto the CPG and the reaction mixture was left for 10 minutes. Afterwards, the deprotection solution was removed with the use of vacuum and the procedure was repeated 3 times.

Deprotection of the oligonucleotides: the 96-well plate containing cleaved oligonucleotides in AMA mixture was sealed with sealing foil and the reaction mixture was left for 2 to 4 hours at room temperature. Afterwards, AMA solution was removed with a plate evaporator (plate temperature around 35 °C). Crude samples were then precipitated from the ethanol.

Where the crude compounds were of insufficient purity, they were purified on the Waters ACQUITY PREMIER HPLC system (ACQUITY PREMIER Oligonucleotide BEH C18 column; 130 Å; 2.1 × 50 mm, 1.7 μm; Waters) at 65 °C with a flow rate of 0.8 mL/min. Eluent A: 0.1 mol/L triethylammonium acetate in water; eluent B: ACN; liquid chromatography peaks were monitored by UV detector at 260 nm.

LIQUID CHROMATOGRAPHY-MASS SPECTROMETRY ANALYSIS OF THE OLIGONUCLEOTIDES. The identity of oligonucleotides was verified by liquid chromatography mass spectrometry (LC-MS) analysis on Waters SYNAPT XS Ion Mobility Time-of-Flight Mass Spectrometer, (ACQUITY PREMIER Oligonucleotide BEH C18 column; 130 Å; 2.1 × 50 mm, 1.7 μm; Waters) at 65 °C with a flow rate of 0.3 mL/min. Eluent A: 7 mmol/L triethylamine (TEA), 80 mM hexafluoroisopropanol (HFIP) in water; eluent B: 3.5 mmol/L TEA, 40 mmol/L HFIP in 50% ACN; gradient 5% to 30% B in 8 minutes. Samples were run in the negative mode (Electrospray ionization) and analyzed as m/z [M]– or [M-H]–. Liquid chromatography peaks were monitored by UV detector at 260 nm.

QUANTIFICATION AND DUPLEXING. Samples were quantified (in triplicate) measuring the absorbance at 260 nm (NanoDrop One, Thermo Scientific), filtered on a Ultrafree-MC Centrifugal Filter (0.22 μm, 5 minutes, 14,000 rpm, Millipore) and duplexed by heating at 95 °C for 5 minutes.

HUMAN TISSUE ACQUISITION. Surplus human saphenous vein was acquired from patients undergoing CABG surgery at the Royal Infirmary of Edinburgh, United Kingdom (East of Scotland Research Ethics Committee, 15/ES/0094). No selection criteria were applied when consenting patients or utilizing tissue, and any existing comorbidities remained unknown to researchers.

HUMAN SAPHENOUS VEIN SMOOTH MUSCLE CELL CULTURE. Isolation of human saphenous vein smooth muscle cells is as described by Southgate et al[41] in 1992. Briefly, vein tissue was manually scraped with forceps to strip the tunica adventitia of fibroblasts and perivascular adipose tissue. The vein was then cut longitudinally and pinned onto Sylgard 184 Elastomer-coated plates (Dow Corning) with the tunica intima facing upward. The intimal endothelial cell layer was removed by gentle abrasion across the surface of the tissue. One-cm strips of tunica media were then peeled from the adventitia and chopped into 1-mm explants using a McIlwain TC752 tissue

chopper (Campden Instruments) across 2 planes at right angles. Tissue explants were then cultured at 37 °C/5% CO_2 in Smooth Muscle Cell Growth Medium 2 (PromoCell, Heidelberg, Germany) with SMC2 media supplement (PromoCell), 10% fetal bovine serum (Gibco, Thermo Fisher Scientific), 2 mmol/L L-Glutamine (Invitrogen, Thermo Fisher Scientific), 50 μg/mL penicillin (Invitrogen, Thermo Fisher Scientific) and 50 μg/mL streptomycin (Invitrogen, Thermo Fisher Scientific). Once vSMCs had grown from tissue explants and were confluent, they were used for downstream experiments. All cells used were between passages 2 and 5.

TRANSFECTION OF HUMAN SAPHENOUS VEIN SMOOTH MUSCLE CELLS AND PROLIFERATION ASSAY. Transient transfection was performed with either lipofectamine RNAiMax (Invitrogen 13778150, Thermo Fisher Scientific) or in vitro JetPEI (Polyplus) following the manufacturers guidelines. A total of 1×10^5 cells were transfected with siRNA to a final dose of 25 nmol/L in 6-well plates, either in Opti-MEM (Thermo Fisher Scientific) when lipofectamine RNAiMax was used as transfection reagent, or in 150 mmol/L NaCl for JetPEI transfections. Six hours post-transfection, cells were quiesced for 48 hours in Dulbecco's Modified Eagle's Medium (DMEM) (Gibco, Thermo Fisher Scientific) supplemented with 50 μg/mL penicillin (Invitrogen, Thermo Fisher Scientific), 50 μg/mL streptomycin (Invitrogen, Thermo Fisher Scientific) and 0.2% [v/v] fetal bovine serum (FBS) (Gibco, Thermo Fisher Scientific) and then stimulated for a further 48 hours with fresh 0.2% FBS DMEM media containing 10 ng/mL IL1α (R&D Systems 200-LA-010) and 20 ng/mL PDGF-ββ (R&D Systems 220-BB-010), and 10 μmol/L 5-ethynyl-2-deoxyuridine (EdU) (Invitrogen A10044, Thermo Fisher Scientific) where proliferation was assessed. After 48 hours, cells were washed once with 1 × PBS, and cells removed from culture plates by trypsinization (Gibco, Thermo Fisher Scientific, Massachusetts, USA) for downstream experiments.

GENE EXPRESSION ANALYSIS BY QUANTITATIVE REAL-TIME POLYMERASE CHAIN REACTION. Total RNA from human saphenous vein smooth muscle cells was obtained using the miRNEasy kit (Qiagen, product number 217084) following the manufacturer's instructions, as well as utilizing the on-column DNAse digest step to ensure complete removal of any genomic DNA. cDNA was then generated using the High-Capacity cDNA Reverse Transcription Kit, following the manufacturer's instructions (Applied Biosystems 4374967). Quantitative real-time polymerase chain reaction (qRT-PCR) was performed using Power SYBR green (Life Technologies) with custom PCR primers (Eurofins MWG) against SMILR and ubiquitin C (UBC) as housekeeper.[36] Gene expression analyses of the SMILR-responsive network were performed using Taqman probes listed in Supplemental Table 2 and Applied Biosystems Taqman GAPDH Control Reagents (Human) (Applied Biosystems 402869). qRT-PCR programs are as follows: 2 minutes at 50 °C, 10 minutes at 95 °C, 40 cycles of denaturation for 15 seconds at 95 °C, and 1 minute at 60 °C. Fold changes were calculated using the $2^{-\Delta ct}$ method. All graphs and statistical analyses were generated using GraphPad Prism version 10.0 (GraphPad Software).

FLOW CYTOMETRY OF EdU-POSITIVE HUMAN SAPHENOUS VEIN SMOOTH MUSCLE CELLS. Cells were fixed in 70% ethanol for a minimum of 24 hours at 4 °C. EdU incorporation was quantified using the Click-iT EdU Alexa Fluor488 Flow Cytometry Assay Kit (Invitrogen C10425, Thermo Fisher Scientific) according to the manufacturer's instructions. Cells were analyzed on a BD LSR Fortessa flow cytometer (BD Biosciences).

MKI67 STAINING OF HUMAN SAPHENOUS VEIN SMOOTH MUSCLE CELLS. Proliferation assays were performed as described, with cells plated on sterile glass coverslips. At the end of the proliferation assay, cells were fixed in 2% PFA for 30 minutes, before being permeabilized with 0.1% TritonX-100 for 20 minutes. Cells were washed 3× in PBS and then blocked with fish serum blocking buffer (Thermo Fisher Scientific 37527) for 1 hour. Cells were then incubated overnight at 4 °C with rabbit α-human Ki-67 (Invitrogen rabbit monoclonal antibody [SP6] #MA5-14520) at 1:500 and mouse antihuman α smooth muscle actin (αSMA) (Dako M0851) at 1:100, diluted in fish serum blocking buffer. Cells were then washed 3× in 1× PBS before goat antirabbit IgG Alexa Fluor 488 (Invitrogen) and goat antimouse IgG Alexa Fluor 647 were added at 1:500 dilution, diluted in fish serum blocking solution. Coverslips were left for 1 hour in the dark, washed 3× in 1× PBS and mounted using ProLong Gold Antifade Mountant with DAPI (Invitrogen, P36935). Slides were then imaged using a Zeiss Axioscan 7 slide scanner (Carl Zeiss AG) with fixed exposure times set between slides for each channel. The percentage of EdU-positive cells amongst 500 DAPI-positive cells was then calculated using QuPath 0.4.3 software.

RNA-SEQUENCING. Deep RNA-sequencing was performed on RNA extracted and DNAse-treated samples using the miRNeasy mini kit (Qiagen) obtained from 5 biological replicates of quiescent, nontransfected (0.2% NT); mock-transfected, IL-PDGF-treated; siNTC-transfected, IL1-PDGF-treated; or BHF7-transfected, IL1-PDGF-treated vSMCs. PolyA-enriched unstranded libraries were prepared by GENEWIZ, Inc and were sequenced with Illumina HiSeq (paired-end 2 × 150 bp). Between 21 million and 53 million paired reads were obtained to analyze protein-coding gene differential expression. Gene quantification (read count and FPKM) was obtained using RSEM (options: -bowtie2 -paired-end),[42] based on GENCODE annotation (Release 38). For both RNA-sequencing experiments, the differential expression was performed utilizing DESeq2.[43] We considered a threshold of absolute fold change ≥1.5 and adjusted *P* value <0.05 to identify significantly differentially expressed genes between 2 conditions. Sample clustering was evaluated using the principal component analysis (PCA) tool available in DESeq2 on the regularized log transformed data. Pathway enrichment analysis was done using the enrichGO, enrichKEGG, and enrichPathway (for REACTOME) functions within clusterProfiler,[44,45] with the gene set of interest (ie, BHF7-induced or repressed genes) compared with a background of expressed genes (FPKM >1 in at least 1 condition). Fisher's exact tests contained within these functions were used to calculate the *P* values.

HUMAN SAPHENOUS VEIN ORGAN CULTURE. Each tissue was cut into 1-cm segments and bathed for 30 minutes at room temperature in PBS containing either unlabeled BHF7, or Cy3-labelled BHF7 at the indicated concentration, either gymnotically (without transfection reagent) or utilizing the transfection reagent in vivo JetPEI (Jet PEI, Polyplus, Strasbourg, France). Tissue sections treated with PEI only were used as control ("mock"). Tissue segments were then washed with PBS, cut longitudinally and pinned onto Sylgard® 184 elastomer-coated (Dow Corning) tissue culture dishes such that the luminal surface of the tissue faces upwards. Tissue segments were then cultured for 7 days in DMEM (Gibco, Thermo Fisher Scientific) supplemented with 50 μg/mL penicillin (Invitrogen, Thermo Fisher Scientific), 50 μg/mL streptomycin (Invitrogen, Thermo Fisher Scientific), and 0.2% [v/v] FBS (Gibco, Thermo Fisher Scientific) and with 10 μmol/L 5-ethynyl-2-deoxyuridine (EdU) (Invitrogen A10044, Thermo Fisher Scientific) where proliferation was analyzed. All tissue samples were cultured at 37 °C/5% CO_2 and media changed every 48 hours. After 7 days of culture, the tissue was halved using a sterile scalpel. One-half of tissue was suspended in 1 mL RNALater (Invitrogen, Thermo Fisher Scientific) and kept at 4 °C for at least 18 hours before tissue lysing and RNA isolation. The second half of tissue was fixed overnight at 4 °C in 4% paraformaldehyde solution before being transferred to 70% ethanol for subsequent histological processing. 5-μm transverse sections of pinned saphenous vein were prepared by using a microtome by standard histological processes.

ANALYSIS OF GENE EXPRESSION IN HUMAN SAPHENOUS VEIN TISSUE. Tissue sections stored in 1 mL RNALater solution were mechanically sheared into smaller segments using a scalpel before being processed using a Qiagen TissueLyser II machine (Qiagen). Tissues were lysed utilizing a single 5-mm stainless steel bead (Qiagen 69989) placed in 700 μL Qiazol lysis reagent (Qiagen 79306) to ensure full tissue disintegration. Tissues were lysed for >5 cycles at 30 Hz for 3 min/cycle, and progression to RNA isolation was only continued upon visual inspection of complete tissue homogenization. RNA was then isolated using the miRNEasy RNA isolation kit (Qiagen, 217084), following the manufacturer's instructions, as well as utilizing the on-column DNAse digest step to ensure complete removal of any genomic DNA. cDNA was then generated using the High-Capacity cDNA Reverse Transcription Kit, following the manufacturer's instructions (Applied Biosystems 4374967). qRT-PCR was performed using Power SYBR green (Life Technologies) with custom PCR primers (Eurofins MWG) against SMILR and UBC as housekeeper.[36] qRT-PCR programs are as follows: 2 minutes at 50 °C, 10 minutes at 95 °C, 40 cycles of denaturation for 15 seconds at 95 °C, 1 minute at 60 °C. Fold changes were calculated using the $2^{-\Delta ct}$ method. All graphs and statistical analyses were generated using GraphPad Prism version 10.0 (GraphPad Software).

PCNA/MYH11 CHROMOGEN STAINING OF HUMAN SAPHENOUS VEIN TISSUE. Transfection experiments were performed as previously described, and tissue sections fixed overnight at 4 °C in 4% paraformaldehyde before being transferred to 70% ethanol and sent to the University of Edinburgh histology services for standard paraffine embedding and sectioning. All tissue slides were deparaffinized using xylene and dehydrated in 100% ethanol. Endogenous peroxidase activity was blocked using 0.3% hydrogen peroxide/methanol solution, and slides were rehydrated using an ethanol dilution series from 95%, 70%, and 50% before being stored in water. Tissue sections were then incubated with mouse-antihuman Proliferating Cell Nuclear Antigen (PCNA) (Dako,

M0879, clone PC10) at 1:100 dilution in TBS + 1% bovine serum albumin (BSA) + 0.1% Tween 20 (pH 7.4-7.6) for 1 hour at room temperature. Tissues were then washed 3× in TBS and incubated with Brightvision antimouse horseradish peroxidase (HRP) secondary antibody (BrightVision, 1-component detection system Goat Anti-mouse HRP, Immunologic DPVM55HRP) for 30 minutes at room temperature. The secondary antibody was developed using HRP magenta (EnVision FLEX HRP Magenta Substrate Chromogen System [Dako Omnis], Agilent DM857) for 5 minutes before stopping the reaction by washing slides in tap water. Tissue sections were then subject to antigen retrieval by boiling in 10 mmol/L sodium citrate, 0.05% tween 20, pH 6.0 solution for 8 minutes in a standard microwave on low power. Sections were left to cool in the buffer for 30 minutes before continuing. Tissues were then incubated with rabbit antihuman myosin heavy chain 11 (MYH11) (Abcam, ab224804, clone SP314) diluted in TBS + 1% BSA + 0.1% Tween 20 (pH 7.4-7.6) overnight at 4 °C. Tissue sections were then incubated with Brightvision antirabbit AP (BrightVision, 1-component detection system goat anti-rabbit HRP, immunologic DPVO55-rHRP-mAP) for 30 minutes at room temperature. The secondary antibody was then developed using HRP Green (PolyDetector HRP Green Kit, BioSB BSB0130) for 5 minutes before stopping the reaction by washing slides in tap water. Tissue sections were then dehydrated in an ethanol dilution series, before a final mount in xylene. Images were acquired using a Zeiss Axioscan slidescanner and all analysis was performed using Zen Blue and QuPath 0.4.3 software. Using QuPath 0.4.3 software, images from a single patient experiment were opened, and file names blinded using the "mask image names" function. Channel colors for both the PCNA and MYH11 signal were defined by drawing a square around a PCNA- or MYH11-positive area and using this signal to define the channel colors. The "create threshold" function was then used, first to define the MYH11-positive tissue, and subsequently to define the PCNA-positive tissue area. Data for proliferation are thus calculated and plotted as "% PCN- positive area amongst MYH11 positive tissue."

FLUORESCENCE IMMUNOSTAINING IN HUMAN SAPHENOUS VEIN TISSUE. Tissue was formalin-fixed and paraffin embedded as described. Tissue sections were permeabilized using 0.5% Triton X/PBS solution (Dow Inc) for 20 minutes, washed 3× with 3% BSA in PBS (Sigma-Aldrich A7030-100G). and then blocked with fish serum blocking buffer (Thermo Fisher Scientific 37527) for 1 hour. Tissue sections were then incubated overnight at 4 °C with myosin heavy chain 11 rabbit antihuman (Abcam, ab224804), at 1:100 dilution, diluted in fish serum blocking solution. Tissue sections were washed 3× in PBS containing 0.1% Triton X-100 before goat antirabbit IgG Alexa Fluor 647 secondary (Invitrogen) was added at 1:500 dilution, diluted in fish serum blocking solution. Slides were left for 1 hour in the dark, washed 3× in 1× PBS and treated with Sudan black stain for 5 minutes to reduce autofluorescence. Finally, slides were mounted using ProLong Gold Antifade Mountant with DAPI (Invitrogen, P36935). Slides were then imaged using a Zeiss Axioscan 7-slide scanner (Carl Zeiss AG) with fixed exposure times set between slides for each channel.

TUNEL STAINING IN HUMAN SAPHENOUS VEIN TISSUE. Paraffin sections were permeabilized using 0.5% Triton X/PBS solution (Dow Inc) for 20 minutes and then washed 3× with 3% BSA in PBS (Sigma-Aldrich A7030-100G). In situ apoptosis detection was performed on saphenous vein tissues using the Invitrogen Click-iT Plus TUNEL Kit (Invitrogen C10617, Thermo Fisher Scientific), following the manufacturer's instructions. Finally, slides were mounted using ProLong Gold Antifade Mountant with DAPI (Invitrogen, P36935). Slides were then imaged using a Zeiss Axioscan 7 slide scanner (Carl Zeiss AG) with fixed exposure times set between slides for each channel. Each image for a given patient was opened as a new project in QuPath 0.4.3 software and image names masked. The TUNEL (AF488) channel was then switched off. Using the "cell counter" tool, ~750 DAPI-positive cells across 3 areas of the tissue were counted. The TUNEL (AF488) channel was then switched on and a second cell count of TUNEL-positive cells was then performed on the first DAPI-positive cell population. The percentage of TUNEL-positive cells amongst the DAPI-positive population was then calculated and plotted. Negative control staining was also performed for each tissue in which the TUNEL antibody was omitted.

BICINCHONINIC ACID PROTEIN ASSAY. Quantification of total protein from each condition was performed using the Thermo Fisher Scientific Micro BCA Protein Assay Kit according to the manufacturer's instructions (Thermo Fisher Scientific). The assay uses bicinchoninic acid (BCA) as the detection reagent for Cu^{+1}, which is formed when Cu^{+2} is reduced by protein in an alkaline environment. A purple-colored reaction product is formed by the chelation of 2 molecules of BCA with 1 cuprous ion (Cu^{+1}). This water-soluble complex exhibits a strong absorbance at 562 nm that is linear with increasing protein

concentrations. Once total protein concentration was established between conditions, equal amounts of protein were added to the Cleaved Caspase-3 enzyme-linked immunosorbent assay (ELISA).

CLEAVED CASPASE-3 LEVELS IN HUMAN SAPHENOUS VEIN TISSUE. Tissue lysates were prepared by first grinding frozen tissue in liquid nitrogen and adding powdered tissue to 1× Cell Extraction buffer, made as described in Abcam ab220655 Human Cleaved Caspase-3 (Asp175) SimpleStep ELISA kit according to the manufacturer's instructions. Quantitative measurement of Cleaved Caspase-3 in BHF7-transfected saphenous vein tissue was measured using Abcam ab220655 Human Cleaved Caspase-3 (Asp175) SimpleStep ELISA kit, according to the manufacturer's instructions. Wavelengths were measured on a BMG Vantastar microplate reader and analysis performed using BMG MARS data analysis software (BMG Labtech).

CLEAVED CASPASE-3 LEVELS IN vSMCs. Cell lysates were prepared using 1× Cell Extraction buffer, made as described according to the manufacturer's instructions. Quantitative measurement of Cleaved Caspase-3 was measured using Abcam ab220655 Human Cleaved Caspase-3 (Asp175) SimpleStep ELISA kit, according to the manufacturer's instructions. Wavelengths were measured on a BMG Vantastar microplate reader and analysis performed using BMG MARS data analysis software (BMG Labtech). vSMCs treated with 100 μmol/L hydrogen peroxide for 48 hours were used as a positive control.

LACTATE DEHYDROGENASE CYTOTOXICITY ASSAY. Changes in cytotoxicity following BHF7 transfection were determined using the Promega LDH-Glo Cytotoxicity Assay, according to the manufacturer's instructions (Promega #J2380). Mock-treated vSMCs treated for 15 minutes with 20 μL/1 mL of 10% Triton X-100 were used as a positive control. Cell culture medium, which was not conditioned by cells, was used to determine background luminescence. Supernatants were collected and stored in lactate dehydrogenase (LDH) Storage Buffer at −20 °C, prepared according to the manufacturer's instructions. Samples were combined with LDH detection reagent, prepared following the manufacturer's instructions, and incubated for 1 hour at room temperature. Luminescence was recorded using a VANTAstar microplate reader (BMG Labtec).

STATISTICAL ANALYSES OF DATA. Graphs are presented as bar charts of mean ± SD with individual datapoints displayed to demonstrate the full distribution of the data. Each colored point represents data from either 1 patient-derived tissue or smooth muscle cell preparation. For qRT-PCR, data are illustrated as relative gene expression after normalization to housekeeping control, as described by Livak and Schmittgen.[46] Statistical tests used to analyze a given data set included paired Student's *t*-tests for within group comparisons, 1-way analysis of variance for comparisons among 3 or more groups and repeated measures analysis of variance or mixed-effects model to account for correlation within a group (eg, longitudinal changes) or single patient (eg, multiple cells), respectively. Dunnett's (comparisons to a control) or Sidak's post hoc test was used to control type I error for multiple pairwise comparisons. All data sets were assessed for normal distribution using a Shapiro-Wilk test. All statistical analyses were performed using GraphPad Prism 10.0. (GraphPad Software)

RESULTS

GENERATION OF A SMILR-TARGETING siRNA LIBRARY. We first created a library of siRNAs targeting the SMILR sequence and assessed the effect of each synthesized siRNA on SMILR expression and vSMC proliferation. To do this, we first identified potential sequences in SMILR suitable for siRNA design. From an original 900 potential sequences spanning across the entire SMILR sequence, we applied selection criteria to focus sequence ranking. Criteria included selecting sequences with a G/C content of between 40% and 60% (to ensure good solubility and synthesis), excluding sequences predicted to have self-complementarity or form hairpins (performed with miRbase[47]) removing sequences predicted to form G-quadruplex structures (avoidance of stretches of 3 or more bases such as CCC or GGG), and finally performing a BLAST search to remove sequences that might have off-target effects. Additionally, criteria such as ones associated with the stability of the 5′ and 3′ ends of the duplex were applied to further narrow down the number of compounds. After these selection criteria were applied, we narrowed our initial 900 sequences to 76, each of which were synthesized and labelled as BHF*n* (**Figure 1A**). A suitable, nontargeting control siRNA (siNTC) was also designed which does not target any sequence in the human genome, but which has the same chemical modification pattern as the BHF*n* library. The identity of all of the synthesized siRNA compounds was confirmed by liquid chromatography mass spectrometry (LC-MS) analysis (an example in Supplemental Figure 1B).

FIGURE 1 **In Vitro Screening of a SMILR-targeting siRNA Library for Optimal SMILR Silencing and Cessation of Smooth Muscle Cell Proliferation**

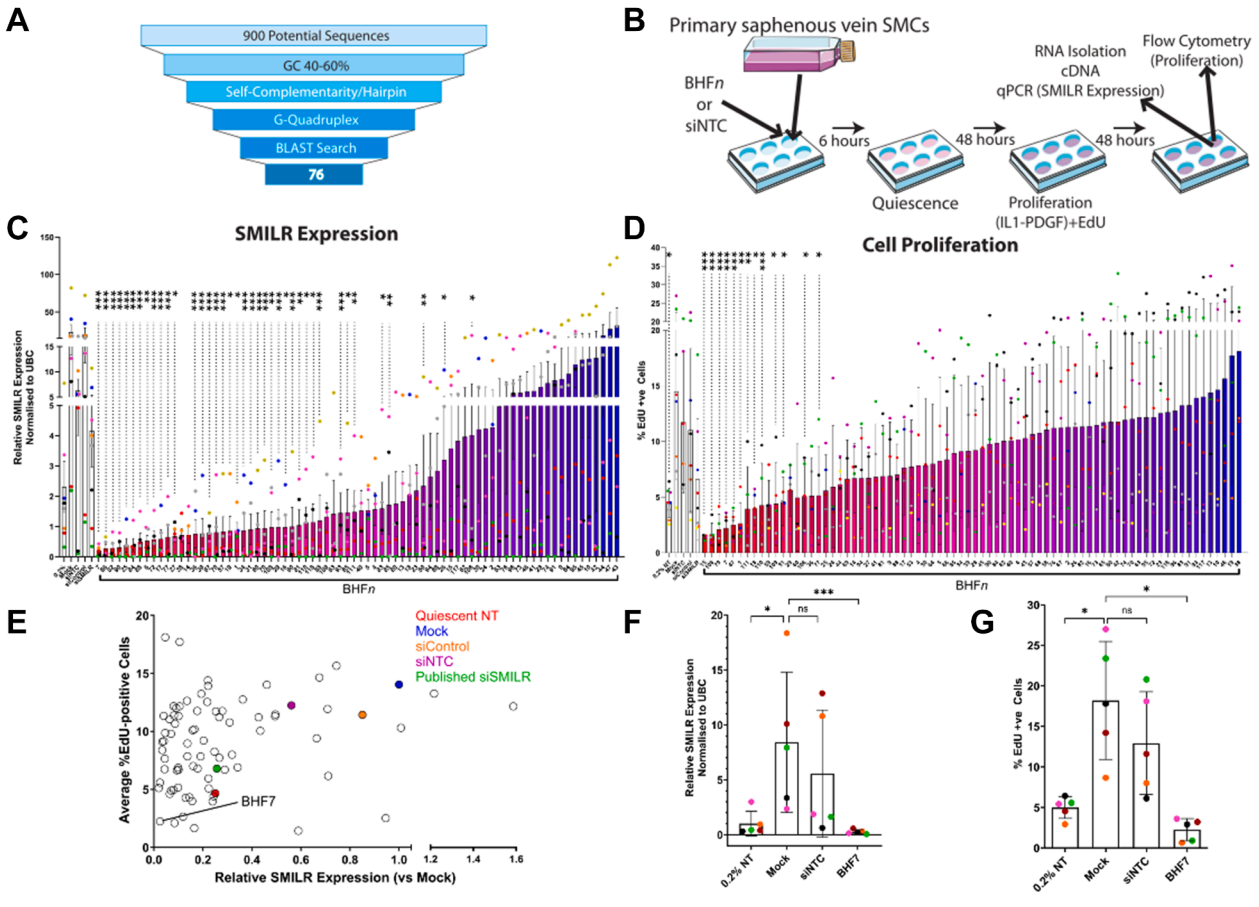

(A) Illustration of the selection criteria used to identify possible sequences within smooth muscle induced long noncoding RNA (SMILR) to generate our siRNA library. From an initial 900 potential sequences, we first removed sequences that did not have a guanine-cytosine content of between 40% and 60%. Next, we removed sequences that had a probability of forming hairpin structures, or to self-anneal. We then removed sequences which were predicted to form G-quadruplex structures, and finally performed a BLAST search to exclude sequences predicted to have off-target effects. We were left with 76 appropriate sequences to target. (B) Overview of the in vitro transfection experiments performed to assess the siRNA library. Created using Servier Medical Art images with modifications. (C) Relative SMILR expression after transfection as indicated and after normalization to UBC. siRNA library is ranked from strongest to weakest effect on SMILR expression. 0.2% = quiescent cells, siControl and siSMILR refer to published siRNA compounds.[36] Each colored dot represents smooth muscle cells derived from a single patient. n = 5 for siRNA; n = 8 for controls. *$P < 0.05$, **$P < 0.01$, ***$P < 0.001$ (written vertically on figure); mixed-effects model with Dunnett's test for multiple comparisons. (D) The % of EdU-positive cells after transfection as indicated. siRNA library is ranked from strongest to weakest effect on proliferation. Each colored dot represents smooth muscle cells derived from a single patient. n = 5 for siRNA; n = 8 for controls. *$P < 0.05$, **$P < 0.01$, ***$P < 0.001$ (written vertically on figure); mixed-effects model with Dunnett's test for multiple comparisons. (E) Scatterplot depicting relative SMILR expression vs mock, nontransfected cells on the x-axis, and the average % of EdU-positive cells on the y-axis. Each data point represents a single siSMILR compound and an average of n = 5 cells derived from patients undergoing CABG surgery. BHF7 was identified as the strongest siRNA at down-regulating SMILR expression and limiting vascular smooth muscle cell proliferation. (F) Individual BHF7 data from (C). Relative SMILR expression after transfection as indicated and after normalization to ubiquitin C (UBC). Each colored dot represents smooth muscle cells derived from a single patient. n = 5, *$P < 0.05$, ***$P < 0.001$; mixed-effects model w/ Dunnett's test for multiple comparisons. (G) Individual BHF7 data from (D). The % of 5-ethynyl-2′-deoxyuridine (EdU)-positive cells after transfection as indicated. Each colored dot represents smooth muscle cells derived from a single patient. n = 5, *$P < 0.05$; mixed-effects model with Dunnett's test for multiple comparisons. siNTC = si-nontargeting control.

MULTIPLE siSMILR COMPOUNDS REDUCE IL1-PDGF-INDUCED SMILR EXPRESSION AND LIMIT PROLIFERATION IN HUMAN SAPHENOUS VEIN-DERIVED SMOOTH MUSCLE CELLS. Each SMILR-targeting siRNA (BHF*n*), and siNTC, was transfected into human primary saphenous vein-derived smooth muscle cells (HSVSMC) (n = 5) to a final dose of 25 nmol/L. This dose is consistent with many in vitro studies[48-50] and is also the dose at which we observed effective SMILR silencing by the previously published unmodified siSMILR.[31,36] To establish the strength of SMILR knockdown from each optimized siRNA, we also

FIGURE 2 BHF7 Reproducibly Blocks SMILR Expression to Limit Proliferation in Primary Patient Saphenous Vein Smooth Muscle Cells

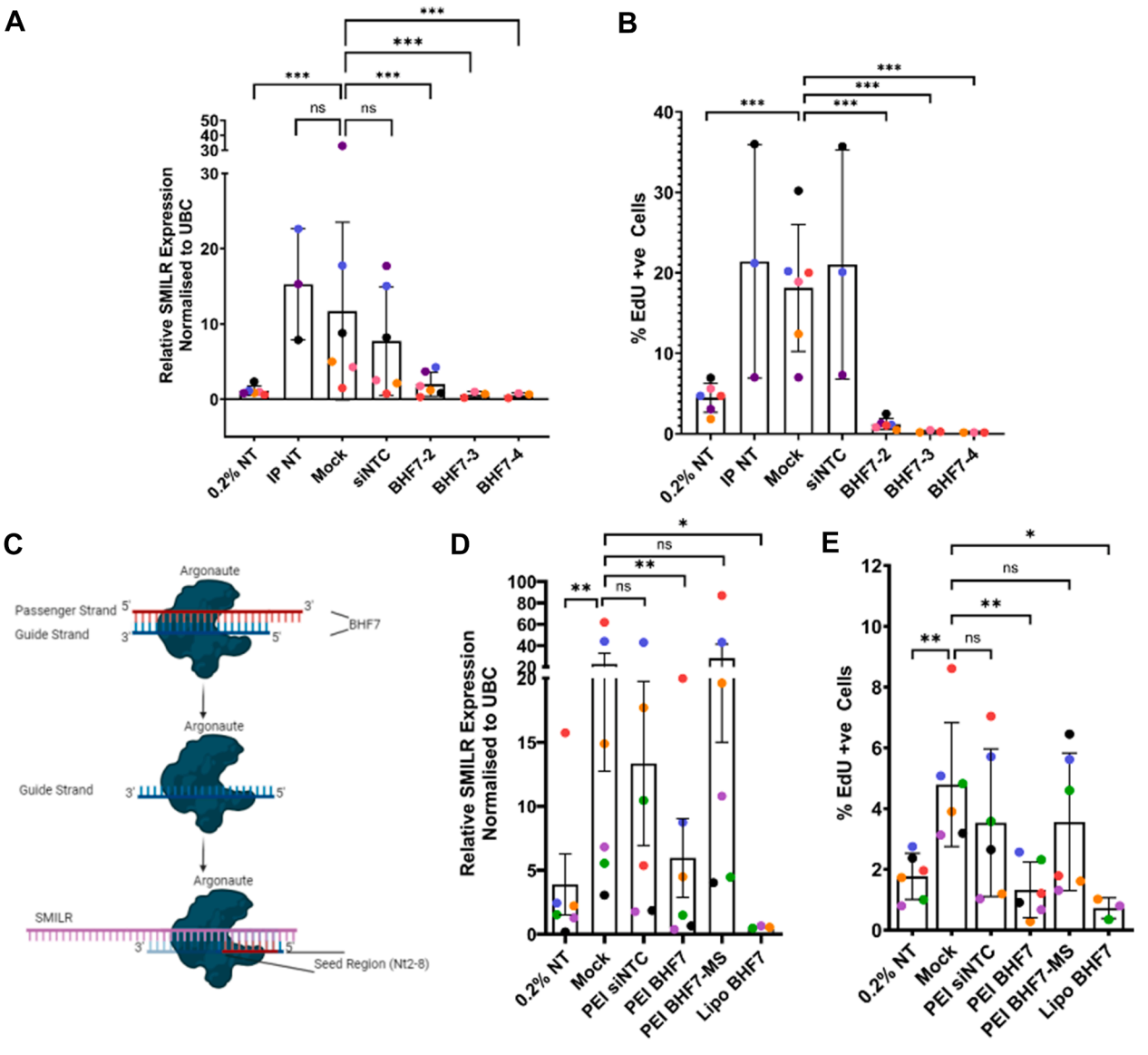

(A) Relative SMILR expression after transfection with new batches of BHF7 (BHF7-2, BHF7-3, BHF7-4) and after normalization to UBC. IP NT refers to nontransfected cells treated with interleukin-1 and platelet-derived growth factor; siNTC refers to cells transfected with control siNTC, mock refers to cells treated with lipofectamine RNAiMax only. Each colored dot represents smooth muscle cells derived from a single patient. n = 3-7. ***$P < 0.001$; mixed-effects model w/ Dunnett's test for multiple comparisons. (B) The % of EdU-positive cells after transfection with new batches of BHF7 (BHF7-2, BHF7-3, BHF7-4). IP NT refers to nontransfected cells treated with interleukin1 and platelet-derived growth factor, siNTC refers to cells transfected with control si-nontargeting control, mock refers to cells treated with lipofectamine RNAiMax only. Each colored dot represents smooth muscle cells derived from a single patient. n = 3-7. ***$P < 0.001$; mixed-effects model with Dunnett's test for multiple comparisons. (C) Schematic depicting the role of the seed region within BHF7 in targeting the RNA-induced silencing complex (RISC) to SMILR. Created using Servier Medical Art images with modifications. (D) Relative SMILR expression after transfection as indicated using either polyethylenimine (PEI) or lipofectamine RNAiMax (Lipo) and after normalization to UBC. Each colored dot represents smooth muscle cells derived from a single patient. n = 7, *$P < 0.05$, **$P < 0.01$; 1-way analysis of variance with Dunnett's test for multiple comparisons. (E) The % of EdU-positive cells after transfection as indicated using either PEI or Lipo. Each colored dot represents smooth muscle cells derived from a single patient. n = 7, *$P < 0.05$, **$P < 0.01$; 1-way analysis of variance with Dunnett's test for multiple comparisons. BHF7-MS = mutated-seed version of BHF7; other abbreviations as in Figure 1.

chose to use the original siSMILR and siControl[36] as additional positive and negative controls, respectively. Both siSMILR and siControl do not possess the enhanced stabilization chemistry modifications used in our optimized siRNA library (Supplemental Figure 1A). We then performed in vitro transfections and the proliferation assay. For every condition, we analyzed in parallel the level of SMILR KD by qRT-PCR and the level of proliferation by flow cytometry (**Figure 1B**).

IL1-PDGF treatment of vSMCs induced a mean 10-fold (range 3.5- to 18-fold) increase in SMILR expression (0.2% vs Mock; $P = 0.019$) which was unchanged by transfection of siNTC ($P = 0.95$) or siControl ($P = 0.99$). Of the 76 SMILR-targeting siRNA developed in this study, 39 reduced SMILR expression relative to mock-treated cells (**Figure 1C**). Importantly, this shows that such an approach of designing a library of compounds targeting discreet regions of interest is a powerful tool where researchers wish to optimize silencing of a particular gene.

From the same transfection experiments, we assessed changes in vSMC proliferation (**Figure 1D**). IL1-PDGF treatment of vSMCs induced an increase in proliferation from a mean of 4.5% EdU-positive cells ($n = 8$) in quiescent nontransfected cells to a mean of 14.5% EdU-positive cells ($n = 8$) in mock-transfected IL1-PDGF-treated vSMCs ($P = 0.014$). This increase in proliferation was unchanged with transfection of either siControl ($P = 0.99$) or siNTC ($P = 0.99$). Thirteen of our SMILR-targeting siRNA caused a reduction in proliferation relative to mock-treated cells (BHF1, BHF7, BHF15, BHF18, BHF31, BHF47, BHF77, BHF79, BHF106, BHF108, BHF109, BHF110, BHF111). We observed that transfection of BHF1, BHF7, BHF15, BHF18, BHF47, BHF59, BHF79, BHF108, BHF109, BHF110 and BHF111 reduced vSMC proliferation to rates below those observed in cells kept in a quiescent state throughout the experiment (0.2% NT).

IDENTIFICATION OF A LEAD siRNA, BHF7, WHICH REPRODUCIBLY SILENCES SMILR EXPRESSION AND LIMITS VSMC PROLIFERATION. To identify a lead siRNA compound from our library which demonstrates maximal SMILR knockdown and cessation of proliferation, we combined our analyses of relative SMILR expression and proliferation to rank our siSMILR library and to identify a top siRNA (**Figure 1E**). This identified BHF7 as the strongest siSMILR compound, both in terms of silencing SMILR expression and limiting vSMC proliferation. Indeed, in our ranking of the BHF*n* siRNA library, BHF7 was the best at knocking down SMILR expression (**Figure 1C**), and fourth best at blocking vSMC proliferation (**Figure 1D**). When the data specifically for BHF7 (**Figures 1C and 1D**) were analyzed in isolation, reductions in both SMILR expression ($P = 0.024$) (**Figure 1F**) and proliferation ($P = 0.003$) (**Figure 1G**) were observed.

To confirm BHF7's role in reducing vSMC proliferation, we used a different measure of proliferation, by performing immunofluorescent staining for Marker of Proliferation Kiel 67 (KI67), a well-established cell proliferation protein.[51] We performed staining in vSMCs which were either quiescent (0.2% NT), treated with IL1-PDGF to induce proliferation or cultured in full SMC media (complete) and were either nontransfected, mock-transfected, or transfected with BHF7 to a final dose of 25 nmol/L, the effective dose ascertained from our in vitro transfection experiments (Supplemental Figure 2). Quiescent, nontransfected vSMCs had low levels of KI67-positive cells, with between 0.19% to 3.9% KI67-positive cells (average 1.9%). When mock-treated vSMCs were induced to proliferate by treatment with IL1-PDGF, we observed an increase in the percentage of KI67-positive cells ($P = 0.017$), which was unchanged relative to nontransfected, IL1-PDGF-treated cells ($P = 0.99$) or to siNTC-transfected vSMCs ($P = 0.77$) but was reduced in BHF7-transfected cells ($P = 0.006$). Collectively, these results demonstrate that BHF7 transfection reduces vSMC proliferation.

To confirm the effect of BHF7 on silencing SMILR expression and limiting proliferation in vSMCs, and to evaluate potential batch-to-batch variation, we independently synthesized 3 additional, identical batches of BHF7, each with the same enhanced stabilization chemistry modification pattern as the original batch. We then repeated our transfection experiments using BHF7-2, BHF7-3, and BHF7-4, again using siNTC as a negative control. We were reproducibly able to demonstrate that BHF7 reduces SMILR expression (**Figure 2A**) (BHF7-2, $P < 0.001$; BHF7-3, $P < 0.001$; BHF7-4, $P < 0.001$) and vSMC proliferation (**Figure 2B**) (BHF7-2, $P < 0.001$; BHF7-3, $P < 0.001$; BHF7-4, $P < 0.001$). These data confirm that BHF7 is a potent siRNA capable of reproducibly silencing SMILR expression and reducing pathologically induced vSMC proliferation.

We used lipofectamine RNAiMax as the transfection reagent. As lipofectamine is not currently

approved for clinical use, we opted to explore alternative delivery methods, which could be used in a clinical setting. Conjugation of organic lipids, such as fatty acids, to siRNA considerably improve siRNA delivery relative to "naked" siRNA.[52-54] We initially conjugated a variety of organic lipids to BHF7, including the fatty acids palmitic acid, oleic acid, and docosanoic acid, as well as cholesterol. However, when in vitro transfection experiments were repeated, we were unable to recapitulate our findings, suggesting that in vitro delivery into human primary vSMCs was insufficient (data not shown). We then opted to abandon tagging of the RNA and instead used the cationic polymer polyethylenimine (PEI) (JetPEI, Polyplus) as transfection reagent, which is being used in several ongoing phase I and II clinical trials of therapeutic oligonucleotides.[55-57] We first confirmed that mock treatment of vSMCs with PEI did not alter the induction of SMILR expression in response to IL1-PDGF treatment (Figure 2D). SMILR expression was increased in mock PEI-treated cells relative to quiescent nontransfected cells (0.2% NT vs mock; $P = 0.001$). This increase in SMILR expression was also not changed when siNTC is transfected into vSMCs using PEI (PEI siNTC) ($P = 0.82$). We then utilized PEI to deliver BHF7 to a final dose of 25 nmol/L into vSMCs (PEI BHF7), and additionally performed transfection experiments using Lipofectamine RNAiMax to permit direct comparison between PEI- and Lipofectamine RNAiMax-mediated delivery (Lipo BHF7). BHF7 delivered using PEI remained able to reduce SMILR expression relative to mock-treated cells ($P = 0.002$), although delivery of BHF7 using Lipofectamine RNAiMax exhibited stronger reductions in SMILR expression ($P = 0.03$) (Figure 2D).

Next, we assessed whether treatment of vSMCs with PEI would impact IL1-PDGF–induced cell proliferation. PEI-only mock-treated vSMCs, again displayed an increase in the percentage of EdU-positive cells in response to IL1-PDGF treatment relative to nontransfected quiescent cells (0.2% NT vs Mock; $P = 0.003$) (Figure 2E). This increase in vSMC proliferation was not changed when siNTC is transfected into cells using PEI (PEI siNTC $P = 0.27$). We noted that the overall level of proliferation was slightly lower than that noted in cells where Lipofectamine RNAiMax was utilized as transfection reagent (mean % EdU-positive cells using PEI ~5% (n = 6), mean % EdU-positive cells using Lipofectamine RNAiMax ~19% (n = 6). Nonetheless, IL1-PDGF–induced vSMC proliferation was reduced when BHF7 was transfected using PEI (PEI BHF7 $P = 0.001$) (Figure 2E). Collectively, these data demonstrate that PEI is suitable as a transfection reagent for BHF7 and does not impede IL1-PDGF induced SMILR expression or cell proliferation.

To confirm that the decreases in SMILR expression and vSMC cell proliferation are mediated through BHF7's SMILR-binding and silencing capability, we synthesized a "seed-mutant" version of BHF7 (BHF7-MS). We targeted nucleotides 2 to 8 of the 5′-end of the guide strand of the siRNA duplex, the region responsible for targeting the RNA-induced silencing complex to its target mRNA to induce its degradation[58] and hypothesized that this mutant-seed version of BHF7 (BHF7-MS) would not function to block SMILR expression or reduce vSMC proliferation (Figure 2C). We used the seed mutant version in our experiments assessing the suitability of PEI as delivery vehicle. BHF7-MS did not reduce SMILR expression relative to mock-treated cells (Figure 2D) ($P = 0.19$). Additionally, BHF7-MS was unable to reduce IL1-PDGF–induced vSMC proliferation (Figure 2E) ($P = 0.26$). Together, these results demonstrate the ability of BHF7 to knockdown SMILR expression and limit vSMC proliferation is mediated through its ability to target RNA-induced silencing complex to SMILR and induce its degradation.

TRANSCRIPTOMIC ANALYSES OF BHF7-TRANSFECTED vSMCs DEMONSTRATES EXPECTED CHANGES TO KNOWN SMILR REGULATED GENES WITHOUT APPARENT TOXIC EFFECT. To assess how transfection of BHF7 into vSMCs alters the transcriptome and to evaluate potential off-target effects, we performed deep RNA-sequencing on human primary saphenous vein-derived smooth muscle cells from 5 patients, nontransfected, mock-treated, or transfected with siNTC or BHF7 to a final concentration of 25 nmol/L. We first used PCA to profile vSMCs transcriptionally which were either mock, siNTC or BHF7-transfected. Our PCA data revealed that vSMCs transfected with BHF7 resulted in wide-spread transcriptomic changes relative to both mock-treated, nontransfected, and siNTC-transfected vSMCs, with 933 genes down-regulated and 386 genes up-regulated in BHF7-treated cells (Figure 3A). These transcriptomic changes contrast the original siSMILR RNA-sequencing data set,[36] where we observed 334 down-regulated and 189 up-regulated genes following down-regulation of SMILR. These differences to the original RNAseq could be explained by

FIGURE 3 **Transcriptomic Profiling of BHF7-Transfected Smooth Muscle Cells Demonstrates that BHF7 Targets a Core Cell Cycle Gene Network**

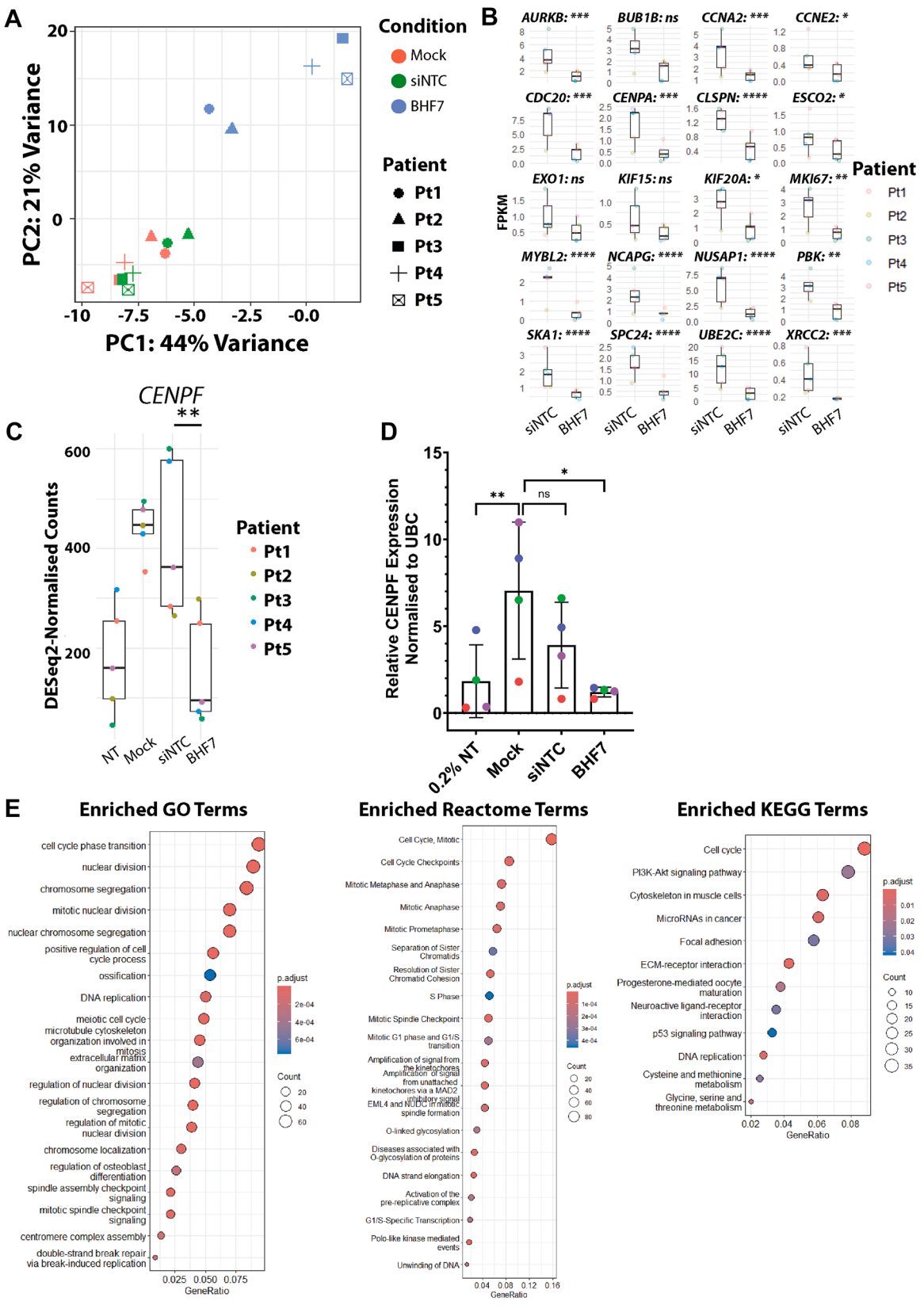

Continued on the next page

the different sequences targeting SMILR in BHF7 and/or the ESC modification of the siRNA.

We previously identified a SMILR-responsive gene network by using a lentivirus to overexpress SMILR and a commercial siRNA to deplete SMILR levels. Analysis of these data revealed a panel of differentially expressed genes, which is enriched in genes associated with the cell cycle and proliferation.[36] To assess whether BHF7 targets the same SMILR-responsive network, we investigated the expression levels of the top 20 differentially regulated genes identified previously. BHF7-transfected vSMCs mirrored the data published previously, with 17 of these genes having significantly reduced expression relative to siNTC-transfected vSMCs (**Figure 3B**). We also confirmed these findings by qRT-PCR (Supplemental Figure 3). In addition, 17.7% of all genes which become repressed by BHF7 transfection (165 genes) have been identified as core cell cycle components.[59]

We previously identified SMILR's mechanism to action in regulating vSMC proliferation.[36] By binding to the mRNA of CENPF, SMILR protects CENPF from Stauffen1-mediated degradation, leading to increased cell proliferation. Concurrently, when SMILR levels are depleted using a commercial siRNA, CENPF levels are also reduced. To verify that the mechanism of action of BHF7 in regulating vSMC proliferation remains the same, we assessed CENPF levels after treatment of vSMCs with BHF7. Analysis of RNA-sequencing demonstrated that CENPF expression is increased in mock-transfected vSMCs treated with IL1 and PDGF relative to nontransfected, quiescent vSMCs (**Figure 3C**). This increase in CENPF expression was unchanged after transfection with siNTC. Transfection of BHF7 resulted in a reduction in CENPF expression levels (**Figure 3C**). We further confirmed these results by qRT-PCR, which again demonstrated that BHF7 reduces CENPF gene expression relative to mock-treated vSMCs ($P = 0.014$) (**Figure 3D**).

To assess biological processes altered by the transfection of BHF7 into vSMCs, we used Gene Ontology (GO),[60,61] Kyoto Encyclopaedia of Genes and Genomes (KEGG) pathway analysis[62,63] and Reactome pathway analysis[64,65] to search for enriched terms amongst all down-regulated genes. Among the 933 BHF7-repressed genes, we found an overwhelming enrichment of terms related to the cell cycle and mitosis across GO, KEGG and Reactome pathway analysis, heavily implicating the cell cycle as the core gene signature altered through the action of BHF7 (**Figure 3E**). We also identified a number of other terms suggesting some repression of cytoskeleton-related processes, extracellular matrix reorganization and muscle-identity programs may occur after BHF7 treatment, which hint at possible wider effects on the repression of phenotypic switching in vSMCs. Conversely, no strong enrichment of any terms was found amongst the 386 BHF7-induced genes. We therefore could not deduce any coordinated biological effect when we search unbiasedly amongst all genes induced by BHF7.

TRANSFECTION OF BHF7 DOES NOT INDUCE CYTOTOXICITY IN HUMAN SAPHENOUS VEIN SMOOTH MUSCLE CELLS. To assess if the introduction of BHF7 into vSMCs causes any cellular cytotoxicity in vitro, both the release of LDH into the culture media and the level of cleaved caspase-3 in cell lysates was measured following transfection of BHF7. We performed the assay after transfection of either siNTC or BHF7 both with and without PEI and collected the cell media to measure LDH activity. We then isolated the cells and prepared a cell lysate to measure the levels of cleaved caspase-3 by enzyme-linked immunosorbent assay (ELISA). We additionally treated cells with TritonX-100 to quantify the total LDH release activity or with 100 μmol/L hydrogen peroxide (H_2O_2) as a positive apoptosis control. BHF7 transfection, both with and without the transection reagent PEI, did not result in an increase of LDH into the media

FIGURE 3 Continued

(A) Principle component analysis of saphenous vein smooth muscle cells transfected with lipofectamine RNAiMax alone (mock), siNTC, or BHF7 to a final dose of 25 nmol/L. (B) BHF7 targets a cell cycle-enriched gene network. Our previous research[36] identified a "SMILR-dependent network." The top 20 differentially-expressed genes identified from this network are enriched for cell cycle-associated genes. This same set of SMILR-dependent genes demonstrate significantly reduced expression when BHF7 is transfected into cells. (C) RNA-sequencing expression analysis of CENPF from NT, mock-transfected, IL1-PDGF-treated cells (mock), siNTC, or cells transfected with BHF7 to a final dose of 25 nmol/L. (D) qRT-PCR validation of RNA-sequencing data for CENPF expression after transfection as indicated. Each colored dot represents smooth muscle cells derived from a single patient. $N = 4$, $^{*}P < 0.05$, $^{**}P < 0.01$, repeated measures analysis of variance w/Dunnett's test for multiple comparisons. (E) Gene ontology (GO), reactome, and KEGG pathway analysis of BHF7-repressed genes reveals a broad network of genes associated with cell cycle progression and mitosis. Abbreviations as in **Figures 1 and 2**.

FIGURE 4 Transfection of BHF7 Into Human Saphenous Vein Smooth Muscle Cells Does Not Induce a Cytotoxic Response

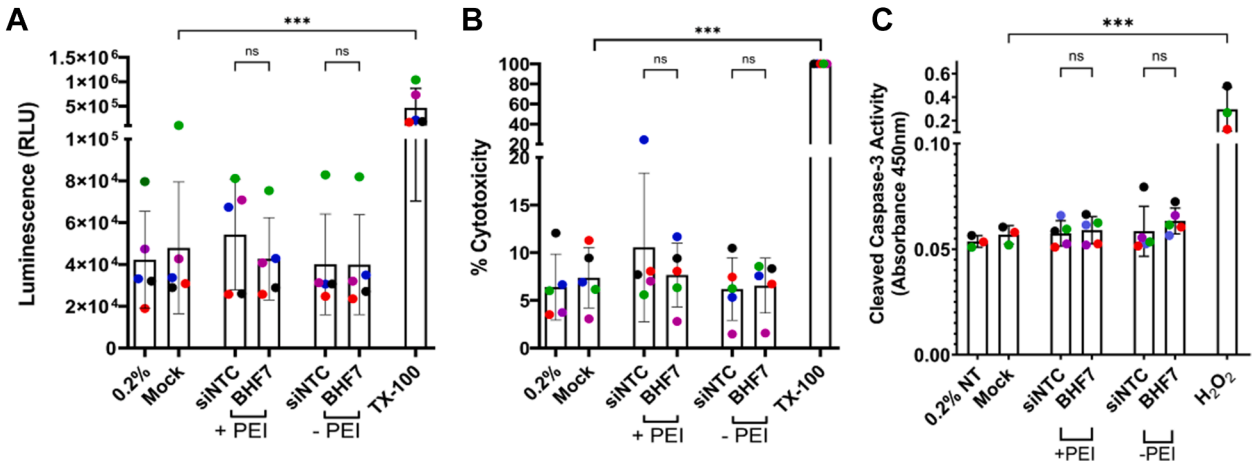

(A) Total amount of lactate dehydrogenase (LDH) protein present in the cell culture media after transfection as indicated. Values are luminescence; cells treated with 10% Triton X-100 for 15 minutes are used as positive control. (B) LDH data presented as % cytotoxicity relative to Triton X-100 treated cells and after correction to media-only LDH levels. (C) Enzyme-linked immunosorbent assay (ELISA) for cleaved caspase-3 activity after transfection as indicated. Cells treated with 100 μmol/L hydrogen peroxide for 48 hours are used as positive control. All experiments n = 3-5 with each colored dot representing human saphenous vein smooth muscle cells taken from a single patient undergoing coronary artery bypass graft surgery. All data analyzed using a mixed-effects model with Šidák multiple comparison's test, ***$P < 0.001$. ns = not significant; RLU = relative light units; other abbreviations as in Figures 1 and 2.

(Figures 4A and 4B) (Raw Luminescence siNTC vs BHF7 +PEI/−PEI, $P > 0.99$; % cytotoxicity siNTC vs BHF7 +PEI, $P = 0.68$; −PEI, $P > 0.99$), or an increase in the total levels of cleaved caspase-3 in vSMCs (Figure 4C) (Absorbance at 450 nmol/L siNTC vs BHF7 +PEI, $P = 0.94$; −PEI, $P = 0.58$). These data demonstrate that when introduced to vSMCs in vitro at a dose of 25 nmol/L, BHF7 does not lead to a breakdown of the cell membrane or result in an increased apoptotic response relative to siNTC transfection.

CY3-BHF7 CAN BE DELIVERED TO MYH11-POSITIVE SMOOTH MUSCLE CELLS IN SAPHENOUS VEIN TISSUE. To assess whether we could deliver BHF7 to human saphenous vein tissue, and specifically to smooth muscle cells, within a clinical timeframe of 30 minutes, a cyanine3-tagged (Cy3) version of BHF7 was synthesized and transfected into saphenous vein tissue at a final concentration of 1 μmol/L, either with or without the use of PEI as transfection reagent. Saphenous vein tissues were then pinned and cultured for 7 days and immunofluorescent staining performed using antibodies against myosin heavy chain 11 (MYH11) to identify the smooth muscle cell layer of the blood vessel (Figure 5). Cy3-BHF7 was detected in tissues, indicating that delivery is possible within a 30-minute window. Cy3-BHF7 was detected in MYH11-positive SMCs (Figure 5), indicating that once in the tissue, BHF7 colocates with vSMCs and acts to block SMILR. BHF7 does not possess any vSMC-targeting elements, and it is therefore probable, and indeed likely, that BHF7 also enters the other cell types present in the vein, including vascular endothelial cells.

BHF7 ATTENUATES SMILR EXPRESSION AND vSMC PROLIFERATION IN HUMAN SAPHENOUS VEIN TISSUE. To test whether BHF7 can have the same effect in clinically relevant tissue, we used the *ex vivo* saphenous vein model,[36,66-68] which uses the same saphenous vein tissue which is grafted into the patient during CABG surgery. This tissue is subject to the same standard surgical manipulation commonly performed during CABG surgery, such as mild distension of the vessel under pressure to assess side-branch leakage and is only acquired following the completion of CABG surgery when the tissue is no longer required. As such, all tissue used is prepared to surgical standards before further experimental manipulation. We performed a 30-minute BHF7 treatment at a final dose of either 250 nmol/L, 500 nmol/L, or 1 μmol/L per cm of tissue to assess delivery to whole saphenous vein tissue (Figure 6A).

FIGURE 5 Cy3-BHF7 Demonstrates Colocalization with MYH11-Positive Smooth Muscle Cells

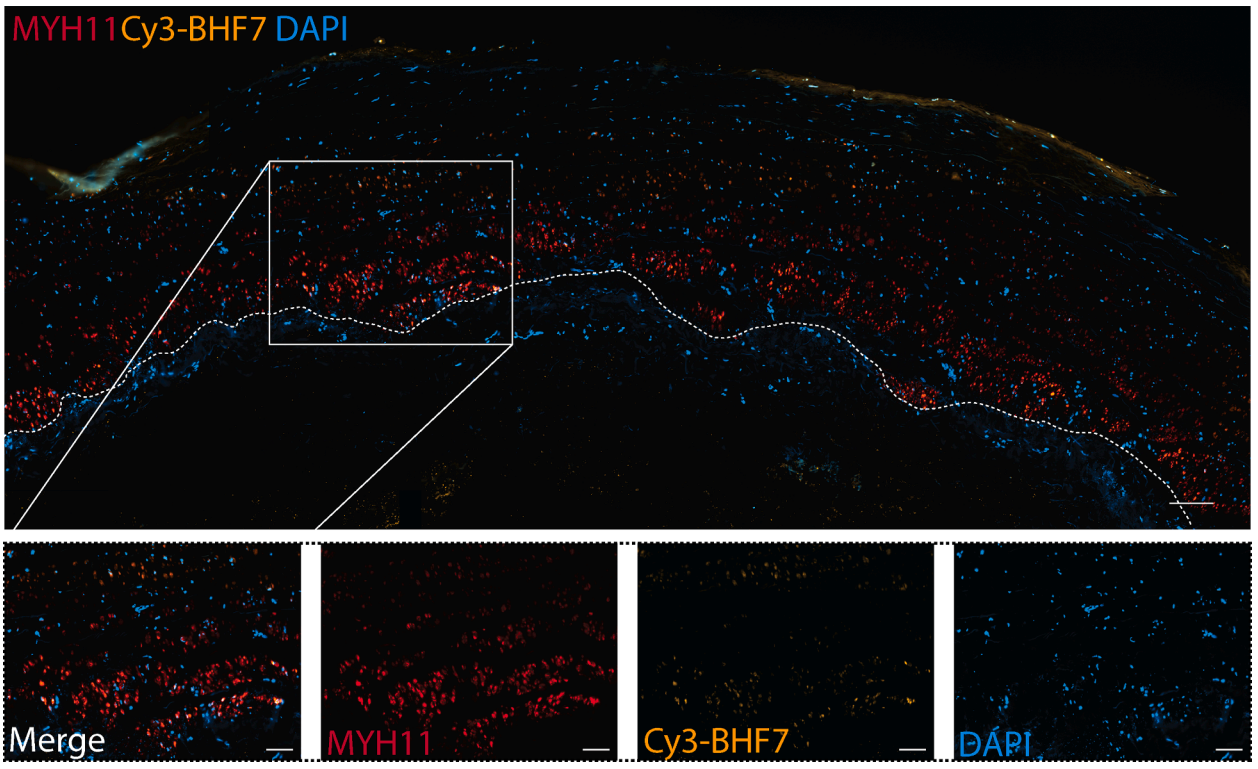

Representative image of human saphenous vein tissue transfected with Cy3-BHF7, cultured for 7 days and stained using an antibody Myosin Heavy Chain 11 (MYH11) (red) and 4′,6-diamidino-2-phenylindole (DAPI) (blue). Dashed lines indicate the boundary between the tunica intima-tunica media. Scale bar on larger images is 100 μmol/L, scale bar on smaller insets is 10 μmol/L.

This model is associated with time-dependent increases in smooth muscle cell proliferation and migration.[66-68] We chose to assess delivery of BHF7 both with and without PEI to see if gymnotic delivery was possible.[69] We first assessed SMILR expression in saphenous vein tissue cultured for 7 days following transfection of BHF7 across a range of doses, either with or without transfection reagent. Relative to nontransfected tissues, transfection of BHF7 at a dose of either 500 nmol/L or 1 μmol/L in the absence of transfection reagent resulted in a decrease in SMILR expression at both 500 nmol/L ($P = 0.012$) and 1 μmol/L ($P = 0.03$), but not at 250 nmol/L ($P = 0.29$) (**Figure 6B**). This concentration window, around 1 μmol/L, is consistent with published reports of oligonucleotide activity when transfected in the absence of any transfection reagent (gymnotically).[70,71] Similarly, transfection of BHF7 using PEI also resulted in a decrease in SMILR expression relative to mock-treated tissue, both at 500 nmol/L ($P = 0.007$) and 1 μmol/L ($P = 0.027$), but not at 250 nmol/L ($P = 0.56$) (**Figure 6C**). From these collective experiments, we define a final dose of 0.5 to 1 μmol/L BHF7 per cm of tissue is sufficient to reduce SMILR expression in intact human saphenous vein tissue.

We then assessed whether delivery of BHF7 to saphenous vein tissue is sufficient to reduce vSMC proliferation in whole vein tissue. We performed immunohistochemical staining for the proliferation marker Proliferating Cell Nuclear Antigen (PCNA), and Myosin Heavy Chain 11, to assess proliferation changes specifically within the smooth muscle cell layer of the vein. We additionally analyzed saphenous vein tissue which was not cultured or transfected—we refer to this as “day 0 NT” as it is processed immediately after acquisition from cardiac theatre. Analysis of tissues demonstrated that there is an increase in PCNA when saphenous vein tissue is cultured to 7 days in the absence of any transfection,

FIGURE 6 BHF7 Can Be Delivered to Human Saphenous Vein Tissue and Block SMILR Expression

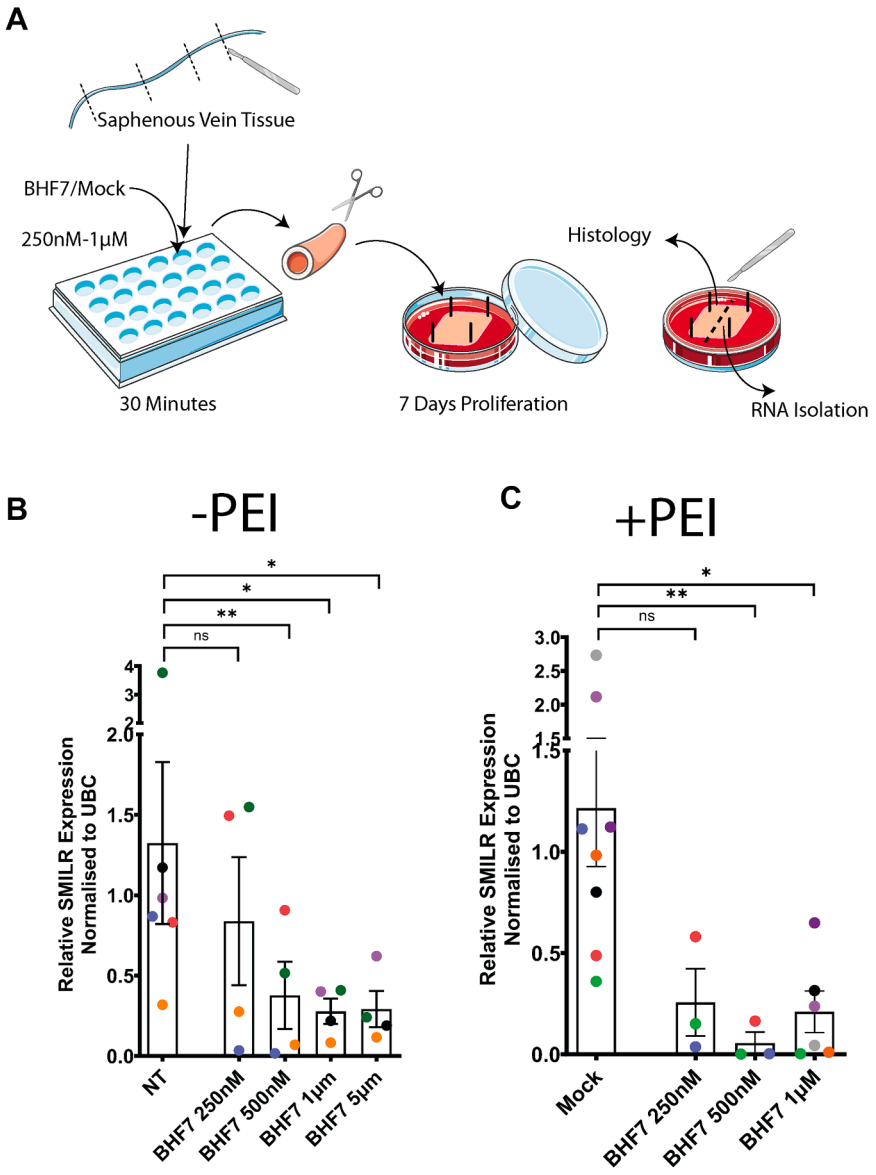

(A) Experimental outline for transfection of BHF7 at various doses into saphenous vein tissue. Created using Servier Medical Art images with modifications. (B) Relative SMILR expression after transfection in the absence of transfection reagent (PEI) as indicated and after normalization to UBC. n = 6 for nontransfected controls, n = 4 for BHF7-transfected tissues, *$P < 0.05$, **$P < 0.01$, mixed-effects model with Dunnett's test for multiple comparisons. (C) Relative SMILR expression after transfection in the presence of transfection reagent (PEI) as indicated and after normalization to UBC. n = 8 for mock-treated tissues, n = 3-6 for BHF7-transfected tissues, *$P < 0.05$, **$P < 0.01$, mixed-effects model with Dunnett's test for multiple comparisons. Abbreviations as in Figures 1 and 2.

relative to day 0 tissue ($P = 0.007$). Further, this analysis illustrated that transfection of BHF7 into saphenous vein tissue at either 0.5 μmol/L ($P = 0.017$) or 1 μmol/L ($P = 0.004$) resulted in a significant decrease in PCNA amongst the MYH11-positive smooth muscle layer (Figures 7A and 7B). We observed similar results when tissue transfection experiments were performed using PEI as the transfection reagent, with BHF7 delivered at a final dose of 1 μmol/L reducing PCNA, and thus vSMC proliferation ($P = 0.009$) (Supplemental Figure 4). Together, these data argue that BHF7 delivered to a final dose of

FIGURE 7 BHF7 Blocks Smooth Muscle Cell Proliferation in Human Saphenous Vein Tissue

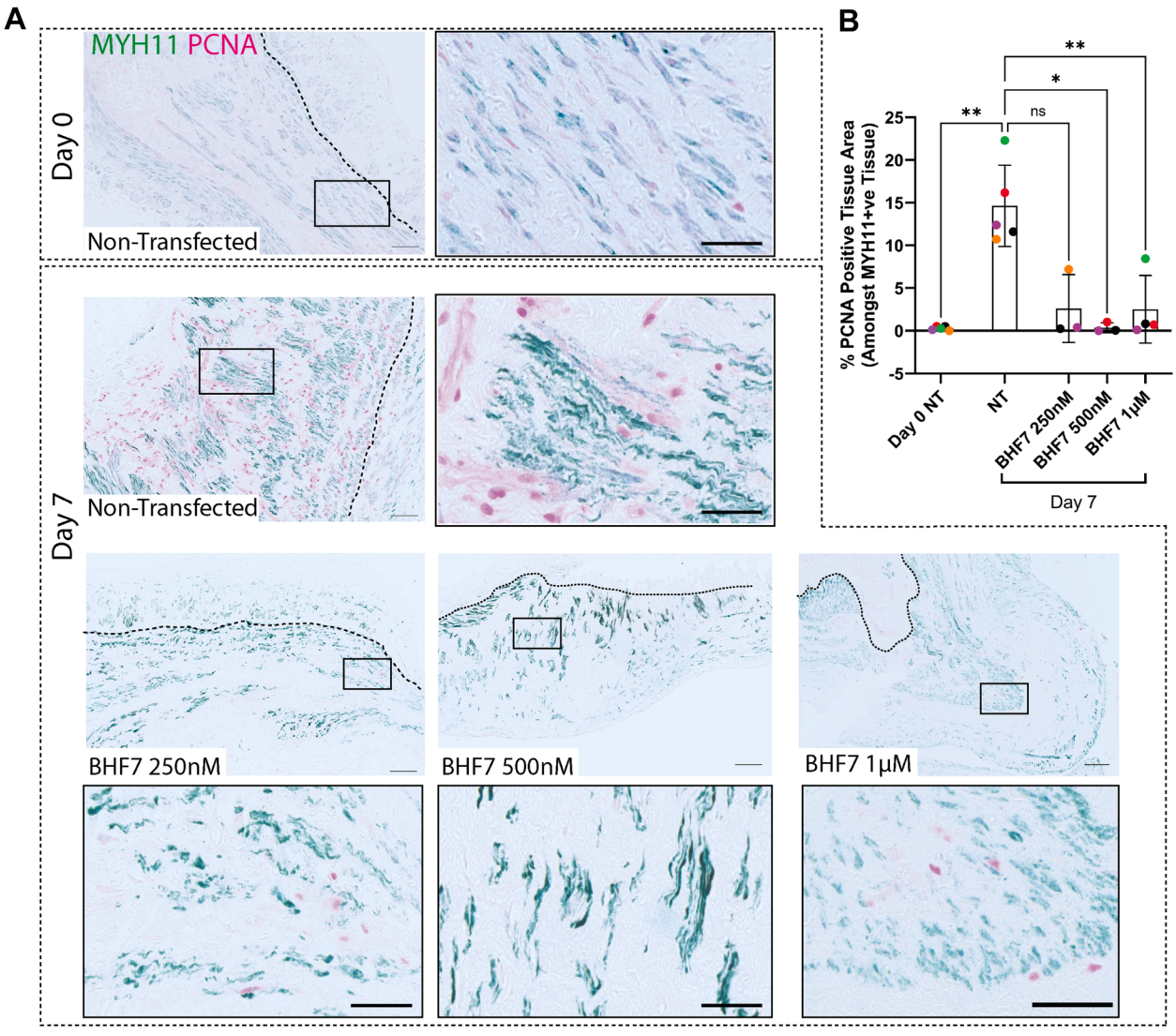

(A) Representative immunohistochemistry of human saphenous vein cultured for either 0 or 7 days after transfection without transfection reagent as indicated. PCNA = proliferating cell nuclear antigen (pink), MYH11 = myosin heavy chain 11 (turquoise). Scale bar is 100 μm (closer insets 50 μm), and dashed lines indicate the boundary between the tunica intima-tunica media. (B) % of PCNA-positive tissue amongst the MYH11-positive medial layer of the vein from days 0 and 7 saphenous vein transfected as indicated, in the absence of transfection reagent (PEI). n = 3-5, *$P < 0.05$; **$P < 0.01$; mixed-effects model with Dunnett's test for multiple comparisons. NT = nontransfected; other abbreviations as in Figures 1 and 2.

0.5 to 1 μmol/L, and both with and without the aid of PEI, is able to reduce smooth muscle cell proliferation in whole saphenous vein tissue.

TRANSFECTION OF BHF7 DOES NOT INDUCE CYTOTOXICITY IN HUMAN SAPHENOUS VEIN TISSUE. To assess whether the introduction of BHF7 into human saphenous vein tissue causes any cytotoxic effects ex vivo, we analyzed DNA fragmentation using the TdT-mediated X-dUTP nick end labelling (TUNEL) assay. The percentage of TUNEL-positive cells did not change between any treatment conditions or by culturing the veins for 7 days (Figure 8A) (day 0 NT

FIGURE 8 **Transfection of BHF7 Into Human Saphenous Vein Tissue Does Not Induce a Cytotoxic Response**

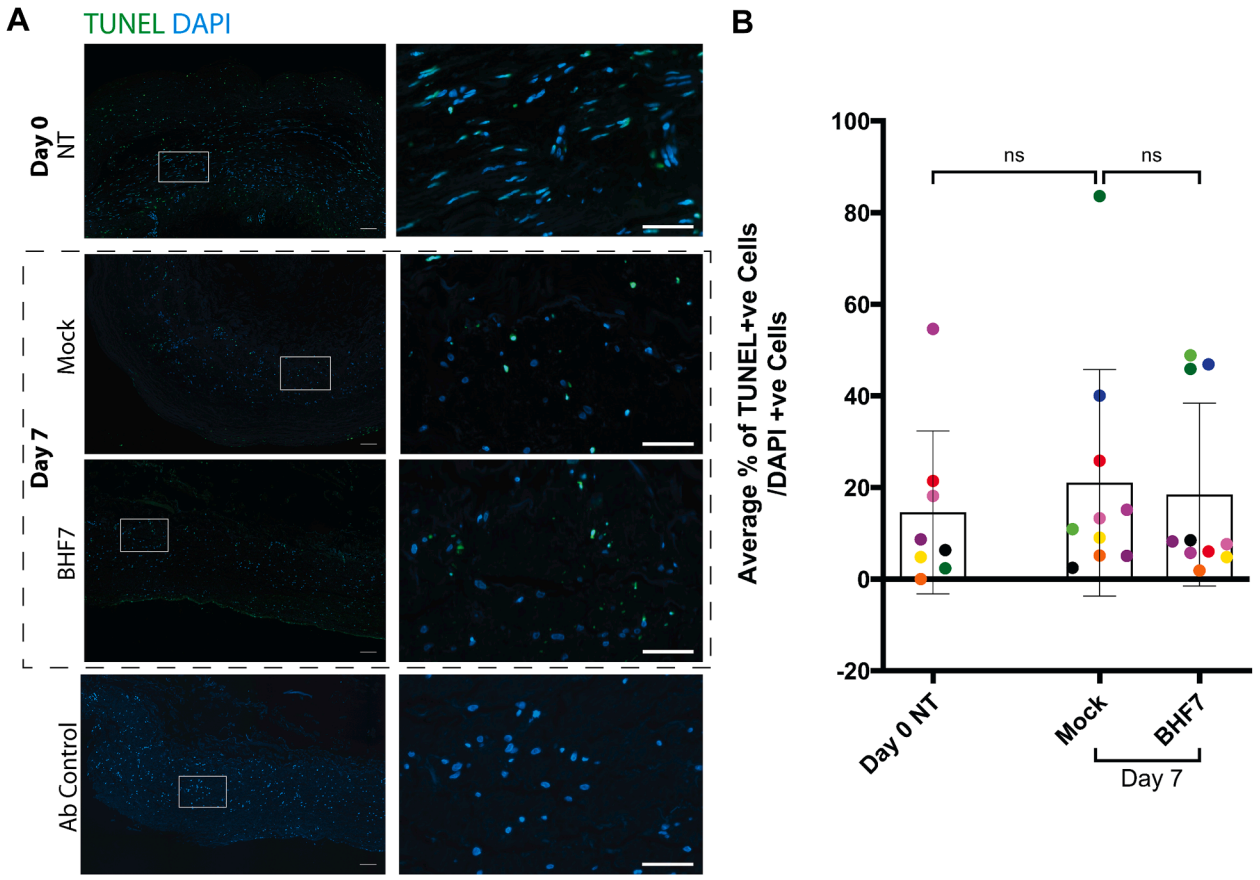

(A) Representative images of human saphenous vein from day 0 (nontransfected) or day 7, either transfected with transfection reagent alone (mock) or transfected with BHF7 to a final dose of 1 μmol/L, and stained for terminal deoxynucleotidyl transferase dUTP nick end labelling (TUNEL) (green) and 4′,6-diamidino-2-phenylindole (DAPI) (blue). Scale bar is 100 μmol/L. B. Average % of TUNEL-positive cells amongst DAPI-positive cells after transfection as indicated, and after tissue culture for either 0 or 7 days. Approximately 750 DAPI-positive cells from 3 distinct areas of the tissue were scored. n = 8-10 with each colored dot representing human saphenous vein from a single patient undergoing coronary artery bypass graft surgery. All data analyzed using a mixed-effects model with Dunnett's test for multiple comparisons, ns = not significant.

vs day 7 mock, $P = 0.94$). Importantly, transfection of BHF7 did not alter the average percentage of TUNEL-positive cells relative to mock treated tissues, either at day 7 ($P = 0.98$) (**Figure 8B**).

To assess cytotoxic effects of BHF7 transfection further, we performed an ELISA to measure cleaved caspase-3 levels in tissue lysates either from day 0 or 7 tissues after treatment with BHF7, or with transfection reagent alone (mock). We observed no differences in cleaved caspase-3 activity between days 0 and 7 ($P = 0.14$). Further, we observed no differences in cleaved caspase-3 activity between mock and BHF7-treated tissues ($P = 0.69$) (Supplemental Figure 5). Collectively, in agreement with our immunohistochemical analyses, these data suggest that treatment of saphenous vein for 30 minutes with BHF7 to a final dose of 1 μmol/L does not induce an increased apoptotic response or result in increased DNA fragmentation relative to untreated or mock-treated tissues.

DISCUSSION

Excessive vSMC proliferation leading to neointimal hyperplasia is a central hallmark of venous bypass graft failure.[6] In this study, we present a preclinical data package describing the potential of BHF7 as a novel siRNA therapeutic, which can be delivered

ex vivo to human saphenous veins as part of CABG surgery to reduce vein graft failure. We synthesized and characterized an siRNA library that can modulate the level of the human-specific long noncoding RNA SMILR and which can reduce pathologically stimulated vSMC proliferation. From this library, we isolated BHF7 as an optimized SMILR-targeting RNA therapeutic which reproducibly down regulates SMILR expression and vSMC proliferation in vitro. While we also noted that BHF7 was not the strongest siRNA at reducing proliferation in our initial screen, the difference in the percentage of EdU-positive cells between BHF15 (the strongest siRNA, at 1.43% EdU-positive) and BHF7 (the fourth strongest siRNA, at 2.24% EdU-positive) is 0.8%. Thus, several compounds are highly effective. BHF7 down-regulates the expression of multiple genes with a common function in regulating the cell cycle and has no apparent cytotoxicity when delivered either in vitro to isolated vSMCs or ex vivo to intact saphenous vein tissue. Finally, BHF7 can be delivered ex vivo to human saphenous vein where it functions to reduce smooth muscle cell proliferation via down-regulating SMILR. Delivery to whole tissue was performed using the same transfection reagent as we did in our in vitro experiments; however, delivery into whole tissue necessitates a much higher dose as the siRNA must traverse multiple barriers to entry to reach its target cells. Importantly, we only expose saphenous vein tissue to BHF7 for 30 minutes to mimic current surgical practice. These data support further studies to ascertain the safety and efficacy of BHF7 as a novel RNA therapeutic delivered ex vivo as part of CABG surgery to improve CABG patency rates. Our RNA-sequencing analysis of vSMCs from 5 patients transfected with BHF7 could not find an enrichment of any specific detrimental pathways amongst all BHF7-regulated genes, including apoptosis or interferon signaling pathways, suggesting BHF7 has minimal off-target effects. It should also be noted that in our initial siRNA selection criteria, we removed sequences predicted to have off-target effects. To assess safety fully however, a clinical study monitoring safety after BHF7 delivery is required.

Targeting vSMC proliferation has been successful in improving clinical outcomes and reducing maladaptive remodeling following vessel stenting by percutaneous coronary intervention[72] but this approach has largely shown disappointing results in failed venous bypass grafts.[73] Despite this, it is important to stress that the proposed approach to target vSMC proliferation ex vivo as a means to reduce venous bypass graft failure remains robust, provided that the proposed modality remains specific to this process only. Substantial preclinical work demonstrated that delivery of edifoligide, a double-stranded oligonucleotide decoy to the E2F transcription factor family,[74,75] could reduce neointimal hyperplasia both in vitro and in several disease animal models.[74,76] Furthermore, re-endothelialization and endothelial cell function was reported to remain unaltered after treatment with edifoligide.[77] Two small clinical trials, PREVENT I[78] and II[79] were then performed, both of which indicated that edifoligide could successfully ameliorate neointimal hyperplasia. However, despite these promising results, 2 phase III clinical trials, PREVENT III[80] and PREVENT IV,[73] disappointingly concluded that edifoligide had no effect on vein graft failure. There are many factors which contributed to these failed phase III clinical trials. Edifoligide was delivered via a pressure-mediated system in which the vein was cannulated at one end and the edifoligide solution infused through the lumen of the vessel. The authors of the PREVENT IV trial noted that the rate of vein graft failure in the study population was higher than reported in other clinical studies.[8,11,81] Second, as edifoligide was designed as a decoy containing the E2F consensus sequence, it inhibits the entire E2F transcription factor family. Subsequent research has revealed that some members of the E2F family inhibit neointimal hyperplasia, and others appear to promote it.[82] Finally, although preclinical results concluded that treatment of edifoligide did not impair re-endothelialization or impair endothelial cell barrier function,[77] conflicting research suggests that E2F function is important for endothelial cell homeostasis[83,84]; therefore, impaired endothelial cell function may have also contributed to the higher rate of vein graft failure. These studies emphasize the importance of targeting smooth muscle cell proliferation with high specificity, without any alteration to other biological processes or to other cell types in the vasculature, and the importance of the physical delivery method to minimize additional damage to the grafted tissue. Given that SMILR expression is, to our knowledge, constrained to proliferating vSMCs, is not expressed in endothelial cells, and whose primary function is to promote proliferation in response to vascular insult, SMILR represents a good target for vein graft failure. Further, we demonstrate that delivery in the absence of any transfection reagent (gymnotic delivery) by simple bathing is effective at transducing human

saphenous vein with BHF7, meaning no risk of addition physical trauma to the tissue exists, as may occur with pressure-mediated delivery. BHF7 is therefore a good candidate to specifically block vSMC-driven neointimal hyperplasia without altering endothelial cell homeostasis.

Clinically, the use of siRNA to modulate gene expression in a given disease context has seen remarkable progress and success.[40] To date, 6 siRNA have been approved by the U.S. Food and Drug Administration and the European Medicines Agency for clinical use: Patisiran (Onpattro),[85-87] Givosiran (Givlaari),[88-91] Lumasiran (Oxlumo),[92] Inclisiran (Leqvio),[93-95] Vutrisiran (Amvuttra),[96] and Nedosiran (Rivfloza).[97] Additionally, Fitusiran[100-102] has, this year, been given FDA approval, with another siRNA therapeutic, Plozasiran,[98,99] expected to be approved for clinical use by the end of 2025. These studies demonstrate the power of siRNA therapeutics to accelerate health care for a wide variety of diseases. Delivery of therapeutic oligonucleotides remains one of the pre-eminent challenges, with most oligonucleotides rapidly cleared from the body without ever entering their target tissues.[103,104] Here, we propose to overcome this problem by delivering BHF7 *ex vivo* to saphenous vein at the time of surgery, immediately before grafting to the heart. To date, we are unaware of any RNA therapeutics used clinically in an ex vivo context, with the exception of chimeric antigen receptor (CAR) T-cell therapies.[105,106] Various studies[73,107-109] and current expert opinion[110] recommend that buffered solutions should be used rather than autologous whole blood or 0.9% saline solutions when storing conduits before grafting. In the present study, we have demonstrated that the pharmacological effect of BHF7 can be achieved by delivering the siRNA in phosphate-buffered saline solution, suggesting it should be possible to recapitulate our experimental procedures in cardiac theatre. Crucially, we also demonstrate that delivery of BHF7 is possible within a 30-minute clinical window. Our proposal therefore does not necessitate a change to current surgical practice in any way and our proposed delivery method is in agreement with current expert opinion.[110]

CONCLUSIONS

In this study, we describe the design and assessment of a SMILR-targeting siRNA library, and identify a single siRNA, BHF7, which reproducibly blocks SMILR expression and significantly limits pathologically-induced vSMC proliferation, with no observed cytotoxic affects. RNA-sequencing experiments demonstrated widespread reductions in the expression of multiple cell cycle and mitosis genes, positioning BHF7 as a novel siRNA therapeutic modality that preferentially regulates a core cell cycle gene network. These data support further clinical studies into the use of BHF7 during CABG surgery, immediately prior to graft implantation as a means to block vSMC proliferation and thus improve CABG failure rates.

DATA AVAILABILITY. RNA-sequencing data have been uploaded to the Gene Expression Omnibus (GEO) database. The data accession number is available upon request.

ACKNOWLEDGMENTS The authors wish to thank Dr Loic Roux, staff at the University of Edinburgh's SURF facility and Flow Cytometry and Cell Sorting facility, and all patients that consented the use of their saphenous vein tissue for this study.

FUNDING SUPPORT AND AUTHOR DISCLOSURES

Dr Baker is funded by a British Heart Foundation Translational award (TA/F/20/210022), a British Heart Foundation Chair of Translational Cardiovascular Sciences (CH/11/2/28733), a British Heart Foundation programme grant (RG/20/5/34796), and Medical Research Council Confidence in Concept grant MC_PC_16043. The Nucleic Acid Therapy Accelerator is funded by MRC grant MC_PC_20061. Dr Newby is supported by the British Heart Foundation (CH/09/002, RG/23/F/22/110093, RE/24/130012), Medical Research Council (MR/Y008944/1, G0701127), and the joint Medical Research Council and British Heart Foundation Centre of Research Excellence in Advanced Cardiac Therapies (MR/Z504658/1, SI/F/24/21170016). All other authors have reported that they have no relationships relevant to the contents of this paper to disclose.

ADDRESS FOR CORRESPONDENCE: Prof Andrew Baker, BHF Centre for Cardiovascular Science, Queens Medical Research Institute, University of Edinburgh, 47 Little France Crescent, Edinburgh EH16 4TJ, United Kingdom. E-mail: andy.baker@ed.ac.uk.

PERSPECTIVES

COMPETENCY IN MEDICAL KNOWLEDGE: Short oligonucleotides that target and modulate RNA have now become a clinically relevant therapeutic modality to treat disease. Advancements in chemical modifications, delivery methods, and targeting motifs have allowed several RNA-based therapeutics to be used in clinical practice, including siRNA-based therapeutic oligonucleotides such as Onpattro (Patisiran), Givlaari (Givosiran), and Oxlumo (Lumasiran). Coronary artery bypass graft surgery remains the gold standard of care in patients with advanced, multi-vessel atherosclerosis and is rightly recognized as a landmark in interventional cardiology. Despite a wealth of progress in vein harvesting techniques, vessel storage and post-operative care, graft re-occlusion has remained a constant burden of healthcare systems for decades, and one that presents with enormous financial and morbidity cost. As ex vivo delivery to the grafted tissue is possible immediately prior to grafting, it is rational and indeed, logical, to maximize the potential of this opportunity by delivering therapeutic modalities specifically to the target tissue, which block pathophysiological processes such as vSMC proliferation and, theoretically, prevent failure from beginning, or at least delay the pathophysiological processes such that healthy remodelling of the vessel is favoured. In this work, we provide evidence that such an approach is feasible through the establishment of BHF7 as a potent anti-proliferative, vSMC-targeting therapeutic.

TRANSLATIONAL OUTLOOK: It remains unknown whether a single-dose delivery of BHF7 at the time of CABG surgery will be sufficient to prevent neointimal hyperplasia; further clinical studies are required to address this. However, we anticipate that the reduction in smooth muscle cell proliferation observed after ex vivo BHF7 treatment in this study would delay SMC proliferation sufficiently that normal, gradual adaptation of the vein to the arterial circulation would be promoted. Even if BHF7 was cleared from tissues within weeks of treatment, this timeframe would be enough for the initial inflammatory response to subside and enable re-endothelialization to occur. Thus, the key factors driving SMC proliferation would be diminished by the time BHF7 is cleared from the tissue. Finally, while delivery of BHF7 during CABG surgery remains our primary aim, pathogenic smooth muscle cell proliferation is an area of unmet clinical need in several other pathologies, including peripheral bypass surgery, vascular restenosis following percutaneous coronary intervention, arteriovenous fistulae, and coronary allograft vasculopathy. Therefore, there exists other clinical opportunities for which intervention using BHF7 as a means to reduce excessive smooth muscle cell proliferation may be a viable approach. Although it is far from clinical practice, the notion of coating coronary stents with siRNA-eluting polymers is under development, and therefore, there exists the possibility of coating coronary stents with BHF7; however, this would require further extensive research. This could open the door for potential secondary BHF7 doses where coronary stenting is performed on failing venous bypass grafts.

REFERENCES

1. Alexander JH, Smith PK. Coronary-artery bypass grafting. *N Engl J Med*. 2016;374:1954–1964.

2. Motwani JG, Topol EJ. Aortocoronary saphenous vein graft disease: pathogenesis, predisposition, and prevention. *Circulation*. 1998;97:916–931.

3. Rectenwald JE, Moldawer LL, Huber TS, Seeger JM, Ozaki CK. Direct evidence for cytokine involvement in neointimal hyperplasia. *Circulation*. 2000;102:1697–1702.

4. Gomez D, Owens GK. Smooth muscle cell phenotypic switching in atherosclerosis. *Cardiovasc Res*. 2012;95:156–164.

5. Owens GK, Kumar MS, Wamhoff BR. Molecular regulation of vascular smooth muscle cell differentiation in development and disease. *Physiol Rev*. 2004;84:767–801.

6. de Vries MR, Simons KH, Jukema JW, Braun J, Quax PH. Vein graft failure: from pathophysiology to clinical outcomes. *Nat Rev Cardiol*. 2016;13:451–470.

7. Goldman S, Zadina K, Moritz T, et al. Long-term patency of saphenous vein and left internal mammary artery grafts after coronary artery bypass surgery: results from a Department of Veterans Affairs Cooperative Study. *J Am Coll Cardiol*. 2004;44:2149–2156.

8. Fitzgibbon GM, Kafka HP, Leach AJ, Keon WJ, Hooper GD, Burton JR. Coronary bypass graft fate and patient outcome: angiographic follow-up of 5,065 grafts related to survival and reoperation in 1,388 patients during 25 years. *J Am Coll Cardiol*. 1996;28:616–626.

9. Sabik JF 3rd, Lytle BW, Blackstone EH, Houghtaling PL, Cosgrove DM. Comparison of saphenous vein and internal thoracic artery graft patency by coronary system. *Ann Thorac Surg*. 2005;79:544–551. discussion 544-551.

10. Harskamp RE, Lopes RD, Baisden CE, de Winter RJ, Alexander JH. Saphenous vein graft failure after coronary artery bypass surgery:

pathophysiology, management, and future directions. *Ann Surg*. 2013;257:824–833.

11. Desai ND, Cohen EA, Naylor CD, Fremes SE, Radial Artery Patency Study Investigators. A randomized comparison of radial-artery and saphenous-vein coronary bypass grafts. *N Engl J Med*. 2004;351:2302–2309.

12. Shah PJ, Bui K, Blackmore S, et al. Has the in situ right internal thoracic artery been overlooked? An angiographic study of the radial artery, internal thoracic arteries and saphenous vein graft patencies in symptomatic patients. *Eur J Cardiothorac Surg*. 2005;27:870–875.

13. Khot UN, Friedman DT, Pettersson G, Smedira NG, Li J, Ellis SG. Radial artery bypass grafts have an increased occurrence of angiographically severe stenosis and occlusion compared with left internal mammary arteries and saphenous vein grafts. *Circulation*. 2004;109:2086–2091.

14. Hess CN, Lopes RD, Gibson CM, et al. Saphenous vein graft failure after coronary artery bypass surgery: insights from PREVENT IV. *Circulation*. 2014;130:1445–1451.

15. Weintraub WS, Jones EL, Craver JM, Guyton RA. Frequency of repeat coronary bypass or coronary angioplasty after coronary artery bypass surgery using saphenous venous grafts. *Am J Cardiol*. 1994;73:103–112.

16. Mohler ER 3rd. Peripheral arterial disease: identification and implications. *Arch Intern Med*. 2003;163:2306–2314.

17. Zacharias A, Habib RH, Schwann TA, Riordan CJ, Durham SJ, Shah A. Improved survival with radial artery versus vein conduits in coronary bypass surgery with left internal thoracic artery to left anterior descending artery grafting. *Circulation*. 2004;109:1489–1496.

18. Cho KR, Kim JS, Choi JS, Kim KB. Serial angiographic follow-up of grafts one year and five years after coronary artery bypass surgery. *Eur J Cardiothorac Surg*. 2006;29:511–516.

19. Lytle BW, Loop FD, Cosgrove DM, Ratliff NB, Easley K, Taylor PC. Long-term (5 to 12 years) serial studies of internal mammary artery and saphenous vein coronary bypass grafts. *J Thorac Cardiovasc Surg*. 1985;89:248–258.

20. Collins P, Webb CM, Chong CF, Moat NE, Radial Artery Versus Saphenous Vein Patency Trial Investigators. Radial artery versus saphenous vein patency randomized trial: five-year angiographic follow-up. *Circulation*. 2008;117:2859–2864.

21. Grondin CM, Campeau L, Lesperance J, Enjalbert M, Bourassa MG. Comparison of late changes in internal mammary artery and saphenous vein grafts in two consecutive series of patients 10 years after operation. *Circulation*. 1984;70:I208–I212.

22. Kulik A, Ruel M, Jneid H, et al. Secondary prevention after coronary artery bypass graft surgery: a scientific statement from the American Heart Association. *Circulation*. 2015;131:927–964.

23. de Scheerder IK, Strauss BH, de Feyter PJ, et al. Stenting of venous bypass grafts: a new treatment modality for patients who are poor candidates for reintervention. *Am Heart J*. 1992;123:1046–1054.

24. Blachutzik F, Achenbach S, Troebs M, et al. Angiographic findings and revascularization success in patients with acute myocardial infarction and previous coronary bypass grafting. *Am J Cardiol*. 2016;118:473–476.

25. Ohri SK, Benedetto U, Luthra S, et al. Coronary artery bypass surgery in the UK, trends in activity and outcomes from a 15-year complete national series. *Eur J Cardiothorac Surg*. 2022;61:449–456.

26. Adnan G, Ahmed I, Tai J, Khan MA, Hasan H. Long-term clinical outcomes of percutaneous coronary intervention in saphenous vein grafts in a low to middle-income country. *Cureus*. 2020;12:e11496.

27. Gallo M, Trivedi JR, Monreal G, Ganzel BL, Slaughter MS. Risk factors and outcomes in redo coronary artery bypass grafting. *Heart Lung Circ*. 2020;29:384–389.

28. Maltais S, Widmer RJ, Bell MR, et al. Reoperation for coronary artery bypass grafting surgery: outcomes and considerations for expanding interventional procedures. *Ann Thorac Surg*. 2017;103:1886–1892.

29. Hawkes AL, Nowak M, Bidstrup B, Speare R. Outcomes of coronary artery bypass graft surgery. *Vasc Health Risk Manag*. 2006;2:477–484.

30. Brown SD, Klimi E, Bakker WAM, Beqqali A, Baker AH. Non-coding RNAs to treat vascular smooth muscle cell dysfunction. *Br J Pharmacol*. 2025;182(2):246–280.

31. Ballantyne MD, Pinel K, Dakin R, et al. Smooth muscle enriched long noncoding RNA (SMILR) regulates cell proliferation. *Circulation*. 2016;133:2050–2065.

32. Schermuly RT, Dony E, Ghofrani HA, et al. Reversal of experimental pulmonary hypertension by PDGF inhibition. *J Clin Invest*. 2005;115:2811–2821.

33. Guan S, Tang Q, Liu W, Zhu R, Li B. Nobiletin inhibits PDGF-BB-induced vascular smooth muscle cell proliferation and migration and attenuates neointimal hyperplasia in a rat carotid artery injury model. *Drug Dev Res*. 2014;75:489–496.

34. Liu W, Kong H, Zeng X, et al. Iptakalim inhibits PDGF-BB-induced human airway smooth muscle cells proliferation and migration. *Exp Cell Res*. 2015;336:204–210.

35. Gong C, Maquat LE. lncRNAs transactivate STAU1-mediated mRNA decay by duplexing with 3′ UTRs via Alu elements. *Nature*. 2011;470:284–288.

36. Mahmoud AD, Ballantyne MD, Miscianinov V, et al. The human-specific and smooth muscle cell-enriched LncRNA SMILR promotes proliferation by regulating mitotic CENPF mRNA and drives cell-cycle progression which can be targeted to limit vascular remodeling. *Circ Res*. 2019;125:535–551.

37. Thakur S, Sinhari A, Jain P, Jadhav HR. A perspective on oligonucleotide therapy: Approaches to patient customization. *Front Pharmacol*. 2022;13:1006304.

38. Foster DJ, Brown CR, Shaikh S, et al. Advanced siRNA designs further improve in vivo performance of GalNAc-siRNA conjugates. *Mol Ther*. 2018;26:708–717.

39. Nair JK, Willoughby JL, Chan A, et al. Multivalent N-acetylgalactosamine-conjugated siRNA localizes in hepatocytes and elicits robust RNAi-mediated gene silencing. *J Am Chem Soc*. 2014;136:16958–16961.

40. Hu B, Zhong L, Weng Y, et al. Therapeutic siRNA: state of the art. *Signal Transduct Target Ther*. 2020;5:101.

41. Southgate KM, Davies M, Booth RF, Newby AC. Involvement of extracellular-matrix-degrading metalloproteinases in rabbit aortic smooth-muscle cell proliferation. *Biochem J*. 1992;288(Pt 1):93–99.

42. Li H. A statistical framework for SNP calling, mutation discovery, association mapping and population genetical parameter estimation from sequencing data. *Bioinformatics*. 2011;27:2987–2993.

43. Love MI, Huber W, Anders S. Moderated estimation of fold change and dispersion for RNA-seq data with DESeq2. *Genome Biol*. 2014;15:550.

44. Alexa A, Rahnenfuhrer J. topGO: Enrichment Analysis for Gene Ontology. 2025. R package version 2.60.1. https://doi.org/10.18129/B9.bioc.topGO

45. Xu S, Hu E, Cai Y, et al. Using clusterProfiler to characterize multiomics data. *Nat Protoc*. 2024;19:3292–3320.

46. Livak KJ, Schmittgen TD. Analysis of relative gene expression data using real-time quantitative PCR and the 2(-Delta Delta C(T)) Method. *Methods*. 2001;25:402–408.

47. Griffiths-Jones S. miRBase: the microRNA sequence database. *Methods Mol Biol*. 2006;342:129–138.

48. Ki KH, Park DY, Lee SH, Kim NY, Choi BM, Noh GJ. The optimal concentration of siRNA for gene silencing in primary cultured astrocytes and microglial cells of rats. *Korean J Anesthesiol*. 2010;59:403–410.

49. Semizarov D, Frost L, Sarthy A, Kroeger P, Halbert DN, Fesik SW. Specificity of short interfering RNA determined through gene expression signatures. *Proc Natl Acad Sci U S A*. 2003;100:6347–6352.

50. Davis SM, Hariharan VN, Lo A, et al. Chemical optimization of siRNA for safe and efficient silencing of placental sFLT1. *Mol Ther Nucleic Acids*. 2022;29:135–149.

51. Scholzen T, Gerdes J. The Ki-67 protein: from the known and the unknown. *J Cell Physiol*. 2000;182:311–322.

52. Biscans A, Coles A, Echeverria D, Khvorova A. The valency of fatty acid conjugates impacts siRNA pharmacokinetics, distribution, and efficacy in vivo. *J Control Release*. 2019;302:116–125.

53. Biscans A, Coles A, Haraszti R, et al. Diverse lipid conjugates for functional extra-hepatic siRNA delivery in vivo. *Nucleic Acids Res*. 2019;47:1082–1096.

54. Hwang J, Chang C, Kim JH, et al. Development of cell-penetrating asymmetric interfering

rna targeting connective tissue growth factor. *J Invest Dermatol*. 2016;136:2305–2313.

55. Casper J, Schenk SH, Parhizkar E, Detampel P, Dehshahri A, Huwyler J. Polyethylenimine (PEI) in gene therapy: current status and clinical applications. *J Control Release*. 2023;362:667–691.

56. Gofrit ON, Benjamin S, Halachmi S, et al. DNA based therapy with diphtheria toxin-A BC-819: a phase 2b marker lesion trial in patients with intermediate risk nonmuscle invasive bladder cancer. *J Urol*. 2014;191:1697–1702.

57. Markowitz J, Shamblott M, Brohl AS, et al. First-in-human stage III/IV melanoma clinical trial of immune priming agent IFx-Hu2.0. *Mol Cancer Ther*. 2024;23:1139–1143.

58. Jackson AL, Burchard J, Schelter J, et al. Widespread siRNA "off-target" transcript silencing mediated by seed region sequence complementarity. *RNA*. 2006;12:1179–1187.

59. Giotti B, Chen SH, Barnett MW, et al. Assembly of a parts list of the human mitotic cell cycle machinery. *J Mol Cell Biol*. 2019;11:703–718.

60. Ashburner M, Ball CA, Blake JA, et al. Gene ontology: tool for the unification of biology. The Gene Ontology Consortium. *Nat Genet*. 2000;25:25–29.

61. Aleksander SA, Balhoff J, Carbon S, et al, Gene Ontology Consortium. The Gene Ontology knowledgebase in 2023. *Genetics*. 2023;224.

62. Kanehisa M, Goto S. KEGG: Kyoto encyclopedia of genes and genomes. *Nucleic Acids Res*. 2000;28:27–30.

63. Kanehisa M, Furumichi M, Sato Y, Matsuura Y, Ishiguro-Watanabe M. KEGG: biological systems database as a model of the real world. *Nucleic Acids Res*. 2025;53:D672–D677.

64. Milacic M, Beavers D, Conley P, et al. The Reactome Pathway Knowledgebase 2024. *Nucleic Acids Res*. 2024;52:D672–D678.

65. Fabregat A, Sidiropoulos K, Viteri G, et al. Reactome pathway analysis: a high-performance in-memory approach. *BMC Bioinformatics*. 2017;18:142.

66. Angelini GD, Soyombo AA, Newby AC. Winner of the ESVS prize 1990. Smooth muscle cell proliferation in response to injury in an organ culture of human saphenous vein. *Eur J Vasc Surg*. 1991;5:5–12.

67. Soyombo AA, Angelini GD, Bryan AJ, Newby AC. Surgical preparation induces injury and promotes smooth muscle cell proliferation in a culture of human saphenous vein. *Cardiovasc Res*. 1993;27:1961–1967.

68. Soyombo AA, Angelini GD, Bryan AJ, Jasani B, Newby AC. Intimal proliferation in an organ culture of human saphenous vein. *Am J Pathol*. 1990;137:1401–1410.

69. Stein CA, Hansen JB, Lai J, et al. Efficient gene silencing by delivery of locked nucleic acid antisense oligonucleotides, unassisted by transfection reagents. *Nucleic Acids Res*. 2010;38:e3.

70. Abewe H, Deshmukh S, Mukim A, Beliakova-Bethell N. Use of GapmeRs for gene expression knockdowns in human primary resting CD4+ T cells. *J Immunol Methods*. 2020;476:112674.

71. Gauthier F, Claveau S, Bertrand JR, Vasseur JJ, Dupouy C, Debart F. Gymnotic delivery and gene silencing activity of reduction-responsive siRNAs bearing lipophilic disulfide-containing modifications at 2'-position. *Bioorg Med Chem*. 2018;26:4635–4643.

72. McFadden EP, Stabile E, Regar E, et al. Late thrombosis in drug-eluting coronary stents after discontinuation of antiplatelet therapy. *Lancet*. 2004;364:1519–1521.

73. Alexander JH, Hafley G, Harrington RA, et al. Efficacy and safety of edifoligide, an E2F transcription factor decoy, for prevention of vein graft failure following coronary artery bypass graft surgery: PREVENT IV: a randomized controlled trial. *JAMA*. 2005;294:2446–2454.

74. Morishita R, Gibbons GH, Horiuchi M, et al. A gene therapy strategy using a transcription factor decoy of the E2F binding site inhibits smooth muscle proliferation in vivo. *Proc Natl Acad Sci U S A*. 1995;92:5855–5859.

75. Hoel AW, Conte MS. Edifoligide: a transcription factor decoy to modulate smooth muscle cell proliferation in vein bypass. *Cardiovasc Drug Rev*. 2007;25:221–234.

76. Ehsan A, Mann MJ, Dell'Acqua G, Dzau VJ. Long-term stabilization of vein graft wall architecture and prolonged resistance to experimental atherosclerosis after E2F decoy oligonucleotide gene therapy. *J Thorac Cardiovasc Surg*. 2001;121:714–722.

77. Ehsan A, Mann MJ, Dell'Acqua G, Tamura K, Braun-Dullaeus R, Dzau VJ. Endothelial healing in vein grafts: proliferative burst unimpaired by genetic therapy of neointimal disease. *Circulation*. 2002;105:1686–1692.

78. Mann MJ, Whittemore AD, Donaldson MC, et al. Ex-vivo gene therapy of human vascular bypass grafts with E2F decoy: the PREVENT single-centre, randomised, controlled trial. *Lancet*. 1999;354:1493–1498.

79. Grube E. *Project of Ex-vivo Vein Graft Engineering via Transfection (PREVENT) II trial*. Anaheim, CA: Paper presented at: American Heart Association Scientific Sessions; 2001.

80. Conte MS, Bandyk DF, Clowes AW, et al. Results of PREVENT III: a multicenter, randomized trial of edifoligide for the prevention of vein graft failure in lower extremity bypass surgery. *J Vasc Surg*. 2006;43:742–751. discussion 751.

81. Widimsky P, Straka Z, Stros P, et al. One-year coronary bypass graft patency: a randomized comparison between off-pump and on-pump surgery angiographic results of the PRAGUE-4 trial. *Circulation*. 2004;110:3418–3423.

82. Giangrande PH, Zhang J, Tanner A, et al. Distinct roles of E2F proteins in vascular smooth muscle cell proliferation and intimal hyperplasia. *Proc Natl Acad Sci U S A*. 2007;104:12988–12993.

83. Spyridopoulos I, Principe N, Krasinski KL, et al. Restoration of E2F expression rescues vascular endothelial cells from tumor necrosis factor-alpha-induced apoptosis. *Circulation*. 1998;98:2883–2890.

84. Goukassian DA, Kishore R, Krasinski K, et al. Engineering the response to vascular injury: divergent effects of deregulated E2F1 expression on vascular smooth muscle cells and endothelial cells result in endothelial recovery and inhibition of neointimal growth. *Circ Res*. 2003;93:162–169.

85. Coelho T, Adams D, Silva A, et al. Safety and efficacy of RNAi therapy for transthyretin amyloidosis. *N Engl J Med*. 2013;369:819–829.

86. Suhr OB, Coelho T, Buades J, et al. Efficacy and safety of patisiran for familial amyloidotic polyneuropathy: a phase II multi-dose study. *Orphanet J Rare Dis*. 2015;10:109.

87. Adams D, Gonzalez-Duarte A, O'Riordan WD, et al. Patisiran, an RNAi therapeutic, for hereditary transthyretin amyloidosis. *N Engl J Med*. 2018;379:11–21.

88. Yasuda M, Gan L, Chen B, et al. RNAi-mediated silencing of hepatic Alas1 effectively prevents and treats the induced acute attacks in acute intermittent porphyria mice. *Proc Natl Acad Sci U S A*. 2014;111:7777–7782.

89. Chan A, Liebow A, Yasuda M, et al. Preclinical development of a subcutaneous ALAS1 RNAi therapeutic for treatment of hepatic porphyrias using circulating RNA quantification. *Mol Ther Nucleic Acids*. 2015;4:e263.

90. Sardh E, Harper P, Balwani M, et al. Phase 1 trial of an RNA interference therapy for acute intermittent porphyria. *N Engl J Med*. 2019;380:549–558.

91. Agarwal S, Simon AR, Goel V, et al. Pharmacokinetics and pharmacodynamics of the small interfering ribonucleic acid, givosiran, in patients with acute hepatic porphyria. *Clin Pharmacol Ther*. 2020;108:63–72.

92. Garrelfs SF, Frishberg Y, Hulton SA, et al. Lumasiran, an RNAi therapeutic for primary hyperoxaluria type 1. *N Engl J Med*. 2021;384:1216–1226.

93. Frank-Kamenetsky M, Grefhorst A, Anderson NN, et al. Therapeutic RNAi targeting PCSK9 acutely lowers plasma cholesterol in rodents and LDL cholesterol in nonhuman primates. *Proc Natl Acad Sci U S A*. 2008;105:11915–11920.

94. Fitzgerald K, Frank-Kamenetsky M, Shulga-Morskaya S, et al. Effect of an RNA interference drug on the synthesis of proprotein convertase subtilisin/kexin type 9 (PCSK9) and the concentration of serum LDL cholesterol in healthy volunteers: a randomised, single-blind, placebo-controlled, phase 1 trial. *Lancet*. 2014;383:60–68.

95. Fitzgerald K, White S, Borodovsky A, et al. A highly durable RNAi therapeutic inhibitor of PCSK9. *N Engl J Med*. 2017;376:41–51.

96. Adams D, Tournev IL, Taylor MS, et al. Efficacy and safety of vutrisiran for patients with hereditary transthyretin-mediated amyloidosis with polyneuropathy: a randomized clinical trial. *Amyloid*. 2023;30:1–9.

97. Baum MA, Langman C, Cochat P, et al. PHYOX2: a pivotal randomized study of nedosiran in primary hyperoxaluria type 1 or 2. *Kidney Int*. 2023;103:207–217.

98. Kenet G, Nolan B, Zulfikar B, et al. Fitusiran prophylaxis in people with hemophilia A or B who switched from prior BPA/CFC prophylaxis: the ATLAS-PPX trial. *Blood*. 2024;143:2256–2269.

99. Srivastava A, Rangarajan S, Kavakli K, et al. Fitusiran prophylaxis in people with severe haemophilia A or haemophilia B without inhibitors (ATLAS-A/B): a multicentre, open-label, randomised, phase 3 trial. *Lancet Haematol*. 2023;10:e322-e332.

100. Young G, Srivastava A, Kavakli K, et al. Efficacy and safety of fitusiran prophylaxis in people with haemophilia A or haemophilia B with inhibitors (ATLAS-INH): a multicentre, open-label, randomised phase 3 trial. *Lancet*. 2023;401:1427-1437.

101. Ballantyne CM, Vasas S, Azizad M, et al. Plozasiran, an RNA Interference Agent Targeting APOC3, for Mixed Hyperlipidemia. *N Engl J Med*. 2024;391:899-912.

102. Watts GF, Rosenson RS, Hegele RA, et al. Plozasiran for managing persistent chylomicronemia and pancreatitis risk. *N Engl J Med*. 2025;392:127-137.

103. Juliano RL. The delivery of therapeutic oligonucleotides. *Nucleic Acids Res*. 2016;44:6518-6548.

104. Dowdy SF. Overcoming cellular barriers for RNA therapeutics. *Nat Biotechnol*. 2017;35:222-229.

105. Lonez C, Bolsee J, Huberty F, et al. Clinical proof-of-concept of a non-gene editing technology using miRNA-based shRNA to engineer allogeneic CAR T-cells. *Int J Mol Sci*. 2025;26(4):1658.

106. Ghobadi A, Bachanova V, Patel K, et al. Induced pluripotent stem-cell-derived CD19-directed chimeric antigen receptor natural killer cells in B-cell lymphoma: a phase 1, first-in-human trial. *Lancet*. 2025;405:127-136.

107. Ben Ali W, Bouhout I, Perrault LP. The effect of storage solutions, gene therapy, and antiproliferative agents on endothelial function and saphenous vein graft patency. *J Card Surg*. 2018;33:235-242.

108. Wilbring M, Ebner A, Schoenemann K, et al. Heparinized blood better preserves cellular energy charge and vascular functions of intraoperatively stored saphenous vein grafts in comparison to isotonic sodium-chloride-solution. *Clin Hemorheol Microcirc*. 2013;55:445-455.

109. Harskamp RE, Alexander JH, Schulte PJ, et al. Vein graft preservation solutions, patency, and outcomes after coronary artery bypass graft surgery: follow-up from the PREVENT IV randomized clinical trial. *JAMA Surg*. 2014;149:798-805.

110. Sandner S, Antoniades C, Caliskan E, et al. Intra-operative and post-operative management of conduits for coronary artery bypass grafting: a clinical consensus statement of the European Society of Cardiology Working Group on Cardiovascular Surgery and the European Association for Cardio-Thoracic Surgery Coronary Task Force. *Eur Heart J*. 2025;46:19-34.

KEY WORDS coronary artery bypass graft, long noncoding RNA, RNA therapeutic, vascular smooth muscle cell

APPENDIX For supplemental figures and tables, please see the online version of this paper.